A review of wire arc additive manufacturing and advances in wire arc additive manufacturing of aluminium

Derekar, K.

Original citation & hyperlink:
Derekar, K 2018, 'A review of wire arc additive manufacturing and advances in wire arc additive manufacturing of aluminium' Materials Science and Technology, vol. 34, no. 8, pp. 895-916.
https://dx.doi.org/10.1080/02670836.2018.1455012

DOI 10.1080/02670836.2018.1455012
ISSN 0267-0836
ESSN 1743-2847

Publisher: Taylor and Francis

This is an Accepted Manuscript of an article published by Taylor & Francis in Materials Science and Technology on 08/04/2018, available online: https://doi.org/10.1080/02670836.2018.1455012

A review of Wire Arc Additive Manufacturing (WAAM) and advances in WAAM of aluminium

K. S. Derekar*[a,b]

[a]*Faculty of Engineering, Environment and Computing, Coventry University, Coventry, UK;* [b]*National Structural Integrity Research Centre (NSIRC Ltd), Cambridge, UK*

*Email: derekar.karan@gmail.com

A review of Wire Arc Additive Manufacturing (WAAM) and advances in WAAM of aluminium

Although Wire arc additive manufacturing (WAAM) has proven its capability of fulfilling demands of production of medium-to-large scale components for automotive and allied sectors made up of aluminium, at present WAAM cannot be applied as a fully-fledged manufacturing process because of practical challenges such as under-matched mechanical properties, presence of large residual stresses and mandatory post-deposition operation for the formed component. This paper is the review of WAAM technology including a brief of WAAM history, status, advantages and constraints of WAAM field. A focus is provided including the efforts directed toward the reduction of porosity, tensile properties, microstructural investigations and other valuable advancements in the field of WAAM of aluminium.

Keywords: aluminium; cold metal transfer (CMT); history; interlayer rolling; microstructure; porosity; Wire arc additive manufacturing (WAAM)

1. Introduction

1.1 Additive manufacturing (AM)

Many researchers (1–3) have predicted the profound role that Additive manufacturing (AM) will have in the manufacturing industry of the future. AM is becoming highly popular due to its numerous benefits that are not only limited to its ability to handle a wide variety of material types varying from metals, polymers, and ceramics; but also because of its ability to produce novel, complex and near net shape parts that eliminate the need for additional tooling and re-fixturing. AM assures single-part assembly or bespoke (4) manufacturing because of the processes capability to reduce overall manufacturing cost by having a focused manufacturing process that reduces task time, material wastage and thus better buy-to-fly ratio (BTF), while enhancing the feedback flexibility to turn feedstock into a structure.

1.2 Wire Arc Additive Manufacturing (WAAM)

British Standard Institute (BSI), International Organization of Standardization (ISO) and American Society for Testing and Materials (ASTM) have jointly defined AM, and the ASTM International Committee F42 has classified AM techniques into the seven different categories. Amongst these, only four methods can produce metallic parts in which only one method can create an additively manufactured shaped component in conjunction with metallic filler addition (see Figure 1). The combination of filler wires being fed into a liquid metal pool created using an electric arc as the heat source that forms an object can be identified as a conventional welding process, such as gas metal arc welding (MIG/MAG) (see Figure 2). A technique of manufacturing of entire component from the deposition of weld metal has been in practice since 1920 which is now been exercised as a Wire arc additive manufacturing (WAAM) technique. The technique has revealed many advantages such as better BTF ratio compared to conventional manufacturing processes, theoretically no dimensional limits for the component manufacturing and economical technique compared to powder-based processes when high cost material is considered.

1.3 Aluminium

The unique property combination of good corrosion resistance, high strength-to-weight ratio and ability to get alloyed with numerous metals and non-metals makes aluminium arguably the most attractive and economical metal that finds widespread applications ranging from transportation, electrical, machinery, consumer durables, building and construction, containers and packaging to name but a few. Regardless of the widespread applications, the welding of aluminium has always been troublesome due to numerous aspects associated with basic material characteristics such as high coefficient of thermal expansion, double solidification shrinkage compared to ferrous metals, formation of a highly retentive oxide film and porosity formation. Solidification cracking adds complexity in welding of aluminium which is greatly related with the alloy composition that indirectly refers the amount of eutectic present at the solidification. Particularly with Al-Cu, Al-Si, Al-Mg, Al-Li and Al-Mg-Si alloys, along with increment in the alloy concentration, crack sensitivity increases until a peak is reached. Beyond this threshold, excess eutectic supports in backfilling of the crack thus reduces the crack sensitivity (Table 1). Alloys 2024 and 7075 are highly susceptible to the solidification cracking. Figure 3 illustrates an example of solidification cracking in aluminium welding. The volatile elements such as magnesium in 5xxx series (major alloying element) alloys volatilises during welding that affects adversely tensile properties of the weld joint.

The effect of raised temperature at heat affected zone (HAZ) is complex. Depending upon the distance from heat source and weld metal, HAZ undergoes recovery, recrystallisation, grain growth, precipitation dissolution and/or reprecipitation. When temperature of an area vicinity to weld metal crosses the solvus temperature of an alloy, localised solidification cracking may occur. The 6xxx and 7xxx series alloys experience dissolution of hardening precipitates (Mg_2Si and $MgZn_2$ respectively) while 2xxx alloys prevail dissolution and reprecipitation (Al_2Cu) reducing overall strength. The area where temperature does not exceed solvus line, partial dissolution and precipitate coarsening may occur. These complexities adversely affect the strength of weld assembly which roughly varies across the weld centreline as shown in Figure 4.

2. Wire arc additive manufacturing (WAAM)

2.1 History of WAAM

Even though the acronym WAAM is being widely accepted as a part of AM terminology over the past 15 years, the actual concept of near net shape manufacturing by welding is almost 100 years old. With the advent of welding technology, many inventors have applied contemporary welding techniques to manufacture different shapes which was acknowledged by several names such as Shape welding (SW), Shape melting (SM), Rapid prototyping (RP), Solid freeform fabrication (SFF), Shape metal deposition (SMD) and 3D Welding. Considering the history on a broader scale, WAAM evolution can be subdivided into three periods, as shown in Figure 5.

As early as 1920, Baker (5) filed a patent on the formation of ‘superposed deposit of metal’ using manipulated the helical path of a fusible electrode to form an ornament shown in Figure 6. After this innovative patent, another patent filed by Shockey (6) described the use of welding for cladding, whereby bead overlapping with a recommended overlap of one-third area of the previously deposited bead by consecutive bead led to the best results. Later, Ujiie (7) demonstrated the technique for the formation of a circular cross-sectional pressure vessel solely by progressive deposition of weld metal (see Figure 7). Ujiie also discussed the machining of the inner and outer layers of the formed part. In the following year, Ujiie (8) focused on a deposition rate and developed a three wire electrode gas metal arc welding (MIG/MAG) technique. In 1983, Kussmaul et al. (9) manufactured shape welded component by Submerged arc (SAW) tandem welding that yielded a 20kg/hr deposition rate. Interestingly, authors discussed tensile and impact behaviour of 10MnMoNi55 shape welded product and highlighted a need development of special filler materials for shape welding. The rapid adoption of shape melting was hampered when a shape melted pressure vessel witnessed a crack failure. Until then, the effect of residual stresses and metallurgical phases on mechanical properties of the shaped part were out of focus and hence later gathered considerable importance on overall quality and integrity of the formed part.

The advancement of computer technology into the manufacturing sector reinvented and bolstered 3D welding. Dickens et al. (10) produced an unsupported wall of carbon steel by the layer-by-layer fashion using on-line point-to-point programming with the robotic GMAW process. An offline monitoring system, developed by Ribeiro and Norrish (11) allowed for the slicing of a computer-aided design (CAD) model to facilitate deposition of weld metal layer-by-layer in a prescribed format to create a desired final shape. In another allied study by Zhang et al. (12), accomplished slicing of the final component into many layers using the Initial graphics exchange specification (IGES) format. Complexity and intricacy of the WAAM technique with respect to operation, material handling, formulation and conceptualization followed a trend of process simplification that allowed inventors to manufacture large shapes such as pressure vessels. After introduction of computer-controlled systems in to manufacturing, the technique had to follow a reinvention curve as the introductory technique was entirely different from traditional manual and machine-controlled processes. Though the advanced testing techniques are helping in producing safer structures, clearing the test criteria is an added complexity. The trend of WAAM development and complexity of the process is graphically presented in Figure 8.

2.2 WAAM-to-date

In the 1990s, Rolls Royce along with Cranfield University showed due interest in the manufacturing of aero engine components using the Shape metal deposition (SMD) technique with Ti-6Al-4V and Inconel 718 alloys. Following the interesting subject, in later years several theoretical and practical modelling approaches were undertaken to study the renewed field of WAAM. Some of the notable studied in recent past has been summarised in Table 2. To understand fundamentals of WAAM, behaviour of single bead multi-layer (open loop) structure is widely studied focusing on numerous aspects such as forming appearance, design, residual stress development and distribution, welding process variations, strategic tool path planning and many more.

2.2.1 Forming appearance

To understand the metal behaviour in layered deposition format and to avoid unwanted defects, parametric study is prime important that incorporates controlled metal deposition at the start and end of a bead as well as controlling bead overlapping. Presence of heat sinks at the start of the weld bead accounts for unrestrained flow of weld metal and wrinkle formation (13,14). To counter this effect and to have smooth part profile, emphasis was placed on developing start and stop strategies. Improved deposition velocity and voltage compared to mean welding parameters with unchanged current at the arc strike and reduced deposition velocity at the arc end has produced an acceptable bead appearance for creation of an open as well as closed loop WAAM structures eliminating bulge at bead start and scallop at bead end (15) (see Figure 9 and Figure 10). One of the studies by Geng et al. (16), minimum angle and curvature radius viable with WAAM is 20º and 10mm respectively when layer width is 7.2mm. Though the study has highlighted an important limitation, the minima are subjected to vary with different bead dimensions and filler metal alloys.

In one of the studies on multi-layer overlapping Ding et al. (17) re-established the critical distance between the centres of adjacent weld beads which is 0.738 times the bead width (w) against the traditional value 0.667w (i.e. overlapping of one third area). As this experimentation does not involve variety of metallic alloys, the result demands for reconfirmation of critical distance value for different materials subjected to the unique material characteristics such as molten metal flowability, wettability, viscosity and surface tension for example, 4xxx series alloys possess greater flowability than 5xxx series. Also considering overall structural integrity of a formed component dilution, penetration and lack of fusion need to be addressed before conclusion.

To avoid the characteristic defect of undulation of weld bead commonly known as humping that can affect WAAM productivity, the travels speed of torch has to be restricted to 0.6m/min as addressed by Adebayo et al. (18). Although the study provides practical applications, in depth understanding of the defect formation using scaled analysis as described by Wei (19), defined mathematical approach confirming Pradtl and Marangoni numbers (20) or Rayleigh's theory of instability (21) for WAAM type deposition could have been valued knowledge. As predicted by Nguyen et al. (22), any technique capable of dissipating or reducing the momentum of the backward flow of weld metal such as reactive shielding gases or specific torch angle suitable for WAAM type deposition can be interesting field of study. Also the correlation between surface tension, effect of volatile elements, power density and distribution, pitch formation and amplitude of humping is the necessary understanding that can help in avoiding humping in WAAM.

2.2.2 Design and residual stress

Analytical, statistical and computational study of residual stress distribution in WAAM component and a substrate is necessary to understand the WAAM system. An addition of metal in a layers adds-up noticeable amount of heat into each layer which induces thermal cycles responsible for expansion and contraction of deposited metal creating large thermal stresses into a WAAM component as well as in a substrate. Understanding of residual stress distribution and accordingly the generation of optimum tool path and build strategy through computer-aided simulation has been exercised (23–26) to minimise residual stresses in a formed component.

Williams et al. (27) proposed the back-to-back building strategy creating two WAAM objects on both sides of the substrate that balances residual stresses and eliminates distortion. Also, symmetrical building is another approach that equally deposits weld metal and thus distributes welding heat on both sides of the predefined plane of the substrate. However, these approaches need computer simulation and practical results for validation. To produce complex shapes with cross-over, corners and junctions, researchers (25,28,29) proposed deposition sequence that can produce acceptable WAAM parts with reduced residual stresses, minimum defects and minimum tool movement (refer Figure 11), thus saving overall operational time. Experimentation by Kazanas et al. (30) resulted in possibility of formation of WAAM walls with varying angles ranging from vertical to horizontal (see Figure 12). Thus, closed hollow 3D shapes can be manufactured using WAAM if appropriate parameters and torch angle is maintained.

2.2.3 Interlayer rolling

Typical problem of formation of coarse columnar centimetre scale β grains in a build direction (refer Figure 13), specifically associate with Ti-6Al-4V alloy in directed energy deposition format, was addressed by the many researchers (31–33). Szost et al. (32) argued that the epitaxial growth of β grains from a partially melted substrate in a specific opposite direction of heat flow occurs without nucleation barrier and undercooling only under specific conditions of matching chemistry of feed and base material, presence of strong thermal gradient and presence of completely liquefied filler metal. The interesting phenomena severely affects directional strength compared to the wrought product (33).

This peculiar problem was well tackled by the introduction of strain at each layer by the application of specific load using rollers (31,34,35). The innovative technique was highly successful in producing roughly randomly oriented grain structure with grain size impressively reduced to 100μm (34) by instigation of dislocations at the wall surface which is acting as a substrate for the next depositing layer that disturbs the grain growth in specific <001> direction. The induced strain has impressive effect of reduction of recrystallisation temperature of β phase. With experimentation Martina et al. (35) stated that the recrystallisation is dependent upon amount of strain rather than the highest temperature reached during layer deposition. Thus, higher the loading pressure, more is the induced strain and dislocations which produces smaller prior β grains (see Figure 14). Also, the strain effect produced by flat rollers was found to have better microstructural properties compared to profiled rollers. In all the studies, however, the authors failed to indicate the amount actual strain value that was introduced into a wall at each layer which is important parameter in developing an object with varying thicknesses and different alloys with diverse strength values. A detailed discussion on the response of aluminium alloys to the interlayer rolling is in section 3.2.

2.2.4 Process variation

Possibility of application of two welding arcs for improved deposition rate is always been an area of interest from industry sector. Researchers experimented deposition of WAAM structure with twin wire GMAW (36) and double electrode GMAW (DE-GMAW) (37,38). In comparison between GMAW and DE-GMAW i.e. GMAW+GTAW (37), later process was found beneficial in terms of smaller volume and dimensions of molten weld pool, lower heat input and lesser average temperature of the solidified weld metal with same deposition rate. Microstructural study which was not part of the research, can be interesting because forced cooling effect produced by relatively less energy input for the same volume of filler metal melting may create highly directional cellular and columnar grains as predicted by constitutional supercooling (39). Comparison of microstructures and mechanical properties of low heat input processes namely cold metal transfer (CMT) and DE-GMAW can benefit advancement of WAAM. Although, simplicity in the formation of functionally graded parts in layer type deposition has been studied (36,40,41), the area is still unattended and needs in depth understanding of fundamental behaviour of filler metals of widely different compositions are mixed using single arc. Even though, the hybrid manufacturing, the concept that involves the addition of metal and subsequent removal of part of it to achieve desired final shape and surface finish, possesses attractive cost advantages and enables interesting real time repairing during manufacturing, the concept is still underdeveloped. Designing of a tool with respect to product shape and respective movement is challenging part of hybrid manufacturing where the shape and size of an intended object is not constant.

2.3 WAAM advantages and challenges

The feedstock material for WAAM i.e. wire shape costs 2-15£/kg for steels and 97-240£/kg for titanium alloys whereas same materials cost 60-93£/kg and 264-685£/kg respectively when powder is considered (2). A wide difference in the cost of raw material makes wire-based technique 2 to 50 times cost efficient than powder-based techniques. Production of titanium component through WAAM can be 7% to 69% cheaper than conventional routes (42). However, such an impressive cost advantage is highly doubted when low cost materials such as steel and aluminium are considered. For intricate aero engine parts, BTF ratio of 30 is not unusual when manufactured from stock. Conversely, when the same parts were manufactured using WAAM, impressive material saving was observed (27), with BTF ratio of 1.2 for high-cost titanium alloy.

Deposition rate approaching 10 kg/h for steels (27,34) is achievable with WAAM which is approximately 16 times higher than powder-based processes that possess maximum deposition rate of 600g/h (43). The reason being wide difference in the shape of a single bead. Powder-based processes reveal bead thickness ranging from few microns to maximum 1mm (44) whereas WAAM processes demonstrate bead height 1-2mm (45,46) which is likely to increase proportionately with deposition rate. Although, higher deposition rate is one of the attractive features of WAAM, unlike low deposition rate process, control over the large liquid weld metal is critical. The solidification of large weld pool in WAAM can be correlated with the conventional casting process experiencing difference in solidification behaviours at the centre and outer periphery.

To achieve high production rate wire feed speed should be kept to an optimum balance, failure to control this favour uncontrolled deposition of weld volumes and subsequently imposes surface roughness that ultimately increases process instability. According to Williams et al (27), the deposition rate needs to be restricted below 4kg/h for steels and 1kg/h for aluminium and titanium alloys to restrict BTF ratio below 1.5. This concludes necessity of machining operation for WAAM when high deposition rate is considered. Thus, WAAM cannot be a conclusive net shape operation for any part production where surface roughness is one of the decisive factors.

Addition of metal layer-by-layer using arc imposes thermal cycles on solidified weld metal as well as in substrate. The effect of heat discharge not only causes partial melting and heat treating of the previously deposited layers but also extends a non-isotherm heat treating effect up to 3 to 4 layers below the deposited bead. The level of this modification being a function of heat input and material thermophysical properties. The expansion and contraction of deposited metal enforced by thermal cycles indicatively and substantially generates residual stresses in a substrate and in formed component. Formation of residual stresses in a component by different means, classification, measuring methods and effect on performance is well addressed by Withers and Bhadeshia (47,48). A neutron diffraction, one of the measurement methods for type I (macro-stresses) residual stresses, recommended by Withers and Bhadeshia (47) was applied for the measurement of residual stresses in an arc-based layer type deposition of Ti-6Al-4V alloys to study the effect of interlayer rolling by Colegroave et al. (31). In without rolling condition, the WAAM wall revealed tensile residual stresses (approx. 500MPa) and was equilibrated by compressive stresses in a substrate while the sample was clamped. However, after unclamping compressive plastic strain in the wall caused upwards bending of a substrate relieving tensile stresses and creating in the baseplate. After rolling, impressive reduction in residual tensile stresses was reported (approx. 150MPa). The experiment also confirmed that stress produced by arc deposition is greater that the stress relaxation offered by interlayer rolling. Figure 15 demonstrates the upward distortion produced in a base plate during production of WAAM part which extends upto 15mm when measured at the edge. The study is in line with the results reported by Colegrove et al. (31) that measures 7mm distortion of baseplate.

In comparison with laser and electron based processes that restricts overall dimensions of an object due to chamber size, WAAM is capable of producing objects without dimensional limits. Thus, high deposition rate and theoretically unlimited metal deposition capability makes WAAM suitable for production of medium to large scale parts. However, larger bead volumes and higher surface roughness compared to powder-based processes (25µm or less cited by Gu (43)) restricts its applications to production of low to medium complex parts.

Mechanical strength of WAAMed products tend to under match the strength requirements of wrought product or filler wire of a similar chemistry. Table 3 briefly reveals the tensile properties of steel, stainless steel and titanium alloys of WAAM parts whilst tested in vertical direction. The tensile properties of WAAM parts are highly directional and dependent upon the deposition pattern followed during an object formation. Thus, the directional tensile properties are always needs to be reported. The grain orientation imparts great influence of tensile properties creating WAAM part stronger in specific direction than the other. Details of microstructural imperfections in

Ti-6Al-4V are discussed in the Section 2.2.3 whereas Section 3.2.3 and 3.2.4 discusses microstructural details and mechanical properties of aluminium alloys.

3 WAAM of aluminium

Porosity in aluminium welding as discussed earlier is highly reviewed major concern and one of the prime factors limiting the expansion and widespread applications of aluminium in WAAM field. Identifying the early stages of investigation, researchers thoughtfully applied low heat input CMT process for WAAM of aluminium. The combined effect of CMT, interlayer rolling and heat treatment on porosity and mechanical properties of aluminium alloys is the area of interest for many researchers. Initially an insight is provided on CMT technique followed by advancement of WAAM of aluminium.

3.1 Cold metal transfer (CMT) technique

The invention of the CMT technique, a variation of GMAW process, that produces good quality spatter-free weld with noticeably less heat input (49,50) compared to traditional GMAW modes is widely noted and well accepted by industries all over the world. An innovative modification in the metal transfer and integrated high speed electronic and mechanical control regulates arc length, method of metal transfer and amount of heat transferred to the base metal causes CMT an uncommon technique. The process basically works on the dip transfer concept. The CMT process is named as cold in the relative terms of welding in comparison to other welding techniques because the process constantly fluctuates between hot and cold phases (high and low current and voltage) averaging relatively less hot. Typical current and voltage variations in CMT process is shown in Figure 16.

To gain the maximum advantage of the CMT, four process variants namely conventional CMT, CMT Pulse (CMT-P), CMT Advanced (CMT-ADV) and CMT Pulse Advanced (CMT-PADV) were developed. Noteworthy advantages of these processes not only include lower thermal input with alteration in electrode burn off rate but also great control over the penetration with high wire melting efficiency and high deposition rate comparable to the conventional GMAW process.

3.1.1 CMT operation

Figure 17 and Figure 18 are the cyclograms of welding current vs voltage variations during conventional dip transfer (CDT) and CMT process respectively. Table 4 differentiates the cycle of operation between the same. The operation of CMT in cyclic order can be categorised into 4 distinct stages as explained below.

(1) Arc burning – An arcing mode, considered as a hot stage in which arc is fully ignited with high current and voltage. A metal at the tip of filler wire is heated to its melting temperature forming a globule at the wire tip.

(2) Arc collapse – In this stage, arc length reduces by feeding a filler wire that touches the molten weld metal extinguishing an arc with the reducing power input creating a cold phase. A globule formed during the previous stage is transferred to the liquid weld pool.

(3) Short-circuiting – A filler wire touches the liquid weld pool however, unlike conventional dip transfer, wire is instantaneously retracted back. Hardly any resistance heating is observed during this stage due to small short-circuiting period enforced by the mechanical retraction of a wire and the maintenance of low current for prescribed short-circuiting period by the advanced electronic circuitry.

(4) Arc re-ignition – Welding current and voltage is raised while retracting filler wire from the weld pool. Because of the raised electrical power, arc is reignited resulting in overall temperature rise forming a hot phase and further same cycle is repeated.

The innovative part of the CMT operation is the mechanical retraction of wire and the control of current at a time of short circuiting that not only avoids unnecessary power and temperature rise but also precisely controls filler metal transfer which greatly enhances metallurgical properties.

3.1.2 Heat input calculation

The heat input calculations using tradition formula (equation 1) which considers average values of current and voltage are not very accurate when pulsing is involved. Hence, revised formula that considers instantaneous values of current and voltage needs to be used that can provide precise value of heat input as displayed in an equation 2 (51,52). The error in the heat input calculation using equation 1 can be 9.1%, 16.6% and -14.6% for MIG/MAG Short Arc Transfer (DC), MIG/MAG Pulse Transfer (DC) and MIG/MAG Pulse (RapidArc) Transfer (DC) processes respectively (53,54).

$$Heat\ input = \frac{Voltage\ x\ current}{Travel\ speed} \qquad \text{Eq. (1)}$$

$$Heat\ input = \frac{\eta \sum_{i=1}^{n} \frac{Ii * Ui}{n}}{Travel\ speed} \qquad \text{Eq. (2)}$$

Where, η is welding process efficiency, *Ii* and *Ui* are the instantaneous current and voltage at each instant of time.

Using the later equation, Cong et al. (50) compared the actual heat inputs of conventional CMT, CMT-P, CMT-ADV and CMT-PADV techniques which were

331.6J/mm, 366.8J/mm, 273.4J/mm and 135.4J/mm respectively (1.2 dia. wire) when wire feed speed and travels speed were unchanged (7.5m/min and 0.5m/min respectively). This emphasises that the increasing pulsing effect reduces actual heat input. In this case, with same deposition rate, the heat inputs of CMT-ADV and CMT-PADV processes are 0.82 and 0.4 times to that of conventional CMT processes. For CDT, heat input using routine welding parameters is normally above 400J/mm however for spray transfer value crosses 1kJ/mm (for 1.2 dia. wire). This clearly demonstrates the importance of heat input calculations using equation 2 and thus explains why the CMT is a low heat input process.This fact impacts significantly when layer type deposition is considered.

3.1.3 Applications of CMT

On account of less possibility of warpage and burn through, CMT has been satisfactorily implemented for welding of aluminium sheets (55) and for low dilution cladding of aluminium alloys (56,57) and nickel-based superalloys (58). Elrefaey (59) noted better mechanical characteristics of 7xxx series aluminium alloys compared to conventional GMAW and GTAW processes. Gungor et al. (60) reported higher yield strength values for 5xxx and 6xxx series alloys when welded using CMT compared to any other welding methods previously addressed.

3.2 Advances in WAAM of aluminium

3.2.1 Application of GTAW

Identifying early need of the capability development, various studies were carried out to build up background allowing discussion on fundamental issues related to WAAM of aluminium. In one of the early studies on applicability of GTAW for WAAM of aluminium using 4043 alloy, Wang et al. (61) discussed suitability of varying polarity GTAW. Researchers described the evidence of fine dendritic structure at the top layer and coarse columnar/cellular grain structure in the middle and the bottom of formed part. Therefore, hardness incremental trend was observed from the bottom and middle layers to the top layer. Focusing on high deposition rate and introduction of CMT technique, research direction was shifted to GMAW process; since then on hardly any study was directed towards application of GTAW for WAAM of aluminium.

3.2.2 Porosity

The porosity formation in heat treatable and non-heat treatable alloys is closely related to the presence of alloying elements. The formation of pores in heat treatable alloy is attributed to the nucleation (during cooling) and dissolution (during heating) of eutectic phases (for example Al_2Cu). In one of the related studies, Gu et al. (51) reported the presence of small pores (5μm to 20μm) in heat treatable alloy which was influenced by interdendritic spaces that forced detachment and flotation pores preventing formation of large pores. Large increase in number of pores after heat treatment was inferred to the vacant sites created by complete dissolution of eutectic phase (Table 5). In non-heat treatable alloys, the presence of volatile material (Mg) and the influence of alloying elements on metal solidification were responsible for pore formation.

3.2.2.1 Porosity reduction using CMT

Porosity formation in aluminium has close relationship with weld penetration, heat input, dendrite growth and shape and size of formed grains (50,62). Cong et al. (62) compared the effects of different CMT techniques such as conventional CMT, CMT-P, CMT-ADV and CMT-PADV on porosity formation (refer Figure 19 for macrograph of weld displaying porosity distribution, Figure 20 for microstructural details and Table 5 for detailed comparison of pore size distribution). Comparatively higher heat input, greater penetration and subsequently formed coarse columnar grains prevented the hydrogen escape in conventional CMT (50,62). This mode revealed large number of pores with pore size varying from 10 to >100µm. It was evident that the coalescence of small pores into large pores were responsible for the formation of large pores with size >100µm.

Comparatively less penetration witnessed by CMT-P decreased the escape distance for hydrogen compared to CMT that supported the evidence of lesser number of pores (50). Also, the presence of no pore over a size of 100µm was attributed to the smaller grain size with CMT-P process. Presence of refined equiaxed grains, lower heat input, shallower penetration and alternating polarities producing oxide cleaning effect in CMT-ADV mode significantly helped hydrogen to escape that revealed no pore with size >50µm. The impressive results were obtained using CMT-PADV process with no pores over a size of 10µm. The technique exhibited combined effect of CMT-P and CMT-ADV processes producing finest equiaxed grain structure and lowest dilution (50,62).

Cong et al. (52) reported the presence of lesser number of pores (refer Table 5) in a block structure compared to wall structure when deposited using CMT-P and CMT-ADV processes. Walled structures showed some of the pores with size >50µm whereas, such large pores were absent in block structures. Also, lower heat input of CMT-ADV revealed lesser number pores than CMT-P in a block structure. The dissipation of heat by conduction in a wall structure is possible only through underlying layers. However, material available in surrounding in a block structure extracts heat increasing cooling rate. Thus, formation of refined and finer microstructure in a block structure was responsible for reduced porosity compared to wall structure (see Figure 21).

3.2.2.2 Porosity reduction by interlayer rolling

The pressure exerted by rolls onto the WAAM bead greatly affects the pore structure. The strain induced by rolling, thus large amount of dislocation and vacancies acts as preferential sites for atomic hydrogen absorption. Gu et al. (51) reported the effect of interlayer rolling and post-deposition heat treatment on porosity evolution on heat treatable and non-heat treatable aluminium alloys. In heat treatable alloy, massive reduction of 68.7% and 99.1% in number of pores and 83.5% and 97.2% in percentage area of pores were documented when 15kN and 30kN loads were applied respectively. The reduction in number of pores was 25.9% and 97.5% and reduction in area percentage was 73.7% and 97% for non-heat treatable alloy for same rolling condition (refer Table 5). Impressively, the size of pores was reduced well below resolving power of available instrument that ideally revels complete elimination of porosity. The effect is also corelated with the grain size reduction with increasing rolling load which is explained in section 3.2.3.

3.2.3 Grain structure

Interlayer rolling mechanism is not only supportive in reducing porosity but also it greatly influences the grain structure. The variation of grain size and grain orientation angle with respect to loading conditions is depicted in Figure 22. In different experiments Gu et al. (63) and Gu et al. (64) reported the effect of interlayer rolling on Al-Cu and Al-Mg-Mn alloy WAAM structure. It can be evidenced from Figure 22 that the increasing loading condition creates smaller grains with low misorientaion angle.

For 5087, in as deposited structure grains with size <5µm existed only 7% whilst grains with size >50µm contributed around 40%. With increasing rolling load, number of grains with size <5µm increased to 16%, 34% and 49% for 15kN, 30kN and 45kN respectively. Subsequently, large grains reduced in numbers showing 0% of grains >50µm for 45kN load. The similar trend of reduction in grain size with increasing load can be clearly seen for Al-Cu alloy where grains with size less than 5µm contributed only 13% in as deposited condition which raised to 77% for 45kN load.

Along with this, it is evidenced that the fraction of small grains boundaries (<15°) gradually increased along with increasing rolling load indicating the formation of large amount of sub grains by splitting of large grains. For both alloys with 45kN load, fraction of small grain boundaries contributed more than 70% of the total volume which was 20% and 6% in as deposited condition for alloys 5087 and 2219 respectively. The effect of grain size reduction on tensile properties and hardness is explained in section 3.2.4.

Cong et al. (52) highlighted the difference in the microstructures of wall and block structures when manufactured from CMT-P and CMT-ADV processes. Wall Structures when manufactured from CMT-P technique, due to heat extraction from substrate, columnar grains formed in bottom part, equiaxed non-dendritic grains found in middle region and top region showed equiaxed dendritic portion. With CMT-ADV process, cellular grains were present in between columnar and equiaxed grains due to lower heat input of CMT-ADV. With block structure, microstructure transition was observed within a single bead where central region revealed equiaxed non-dendritic structure and columnar grains in outer part due to faster heat extraction at adjacent area when CMT-P was used. However, CMT-ADV process exhibited equiaxed dendritic zone in outer part. The results obtained from MIG/MAG process i.e. by application of

CMT are in conjunction with the outcomes reported by Wang et al. (61) using VP-GTAW as mentioned in Section 3.2.1. The microstructural details are in conjunction with the porosity reduction as explained in Section 3.2.2.1.

3.2.4 Tensile properties and microhardness

Introduction of large number of dislocations into a WAAM object by rolling and formation of small sized grains greatly enhance tensile properties. The recrystallisation offered by cyclic heating may release strains and dislocations. However, this is not enough to nullify the entire effect induced by rolling and thus considerable density of dislocations remain induced (51) in the interlayer rolled object favouring the tensile strength increment. Table 6 describes the effect increasing load of interlayer rolling on tensile properties and elongation of heat treatable and non-heat treatable aluminium alloys. An approximately linear trend can be seen for incremental tensile strength for increasing rolling loads.

In case of heat treatable alloys, repeated thermal cycles analogous to the annealing and aging heat treatment produced eutectic phases. However these precipitates were inactive in the strength improvement due to their large size and less in numbers (63) which creates weak resistance to dislocation movement. When rolling was applied to these alloys, formed eutectics fractured into smaller sizes depending upon applied load and after heat treatment uniform distribution of eutectics with refined smaller size grains were optioned (63) that greatly enhanceed tensile properties. Interestingly, the tensile properties of heat treated and rolled+heat treated samples showed comparable tensile properties however, grain size of the rolled specimen remained approximately half to that of without rolled specimens which was ascribed to the splitting of coarse grains and emergence of sub-grains due to induced strain by the roller (see Table 6 and Section 3.2.3). In case of 5087, the major strengthening mechanisms are high density dislocations led by deformation, sub-grains produced due to rolling load (see section 3.2.2) and grain refinement. An interesting outcome reported by Geng et al. (16) in which researchers mentioned isotropy in tensile properties when specimens tested parallel and perpendicular direction of the deposition. Conversely, anisotropy was observed when specimens were tested in parallel and perpendicular direction of the grain texture. Thus, tensile strength in perpendicular direction of grain texture was higher than parallel directional properties. This fact is important while designing a component for practical application.

As expected, irrespective of alloy type, a linear trend can be seen between hardness and rolling load (refer Figure 23). As experimented by Gu et al. (64) hardness increment was 14.8%, 27% and 40% compared with as-deposited for 15kN, 30kN and 45kN rolling loads respectively for alloy 5083. Considering 2319 filler wire the incremental values were 14.2%, 33% and 52.8% (65) for the same loading conditions. This implies WAAM parts produced with proper operation can possess equivalent or even higher properties than respective wrought products (see Table 6) and thus, there is close possibility of replacing wrought product with comparable WAAM products in near future.

3.2.5 Chemical composition

To tackle metallurgical issues and reshape the grain structure favourable for the new solidification pattern of WAAM, alteration of chemical composition of filler wire becomes crucial factor. One of the examples of specially designed alloy for 3-D printing is AlMgSc-based corrosion resistant Scalmalloy (66) that eliminates the problems related to the presence of Mg such as spinel formation ($MgAl_2O_4$) and witnesses reduced wettability and vaporization of Mg. Interestingly Scalmalloy displays very good combination of mechanical properties such as high ductility and specific strength comparable to titanium.

Fixter et al. (67) studied the suitability of aluminium 2xxx series alloys focusing on hot crack susceptibility and amount of Mg present in an alloy. Surprisingly, authors found 2024 wire deposition, earlier considered as an unweldable composition, suitable for WAAM. The tensile properties of 2024 (see Table 6) were comparable with respective wrought part. This clearly highlights the fact that weldability of an alloy cannot be considered as a governing criterion for selection of a specific filler metal composition for WAAM application. Future experimental investigations are recommended to assess applicability of other metal alloys to WAAM.

3.2.6 Single step forming

Although, the interlayer rolling process has positively influenced WAAM of aluminium, the process suffers from limitations such as time-consuming process and difficultly in application for formation block structure. An idea of replacing the interlayer rolling with a single step forming process such as bending and forging as an extension of WAAM was emerged (68). Following the formability check by conventional compression test, researchers noted ductile and isotropic nature of WAAM part and through finite elemental analysis study. The authors provided positive results for the application of forming operation that will provide sufficient strain hardening along with the elimination of porosity. Even though there is likelihood of adoption this innovative concept, the results of actual experimentation are absent. Also, the operational feasibility of the introduction of a forming step as an extension of WAAM in the present industrial environment is the major concern where the final shape of component becomes a decisive factor.

3.2.7 Use of other techniques

Despite the CMT technique being widely accepted and studied, potential of other techniques based on short-circuiting metal transfer, similar to CMT such as Pulse multi-control (PMC), Low spatter control (LSC) and Synchrofeed are worth to consider at the development stage of WAAM of aluminium. Unfortunately, hardly any literature available other than CMT discussing its applicability to WAAM.

4 Conclusion

The growing market demands of aluminium products mainly high strength alloys in automobile and aerospace could be satisfactorily fulfilled using WAAM as an economical next-generation option. GMAW based CMT variants have been widely applied and studied as a competent technique for WAAM of aluminium. Elimination of porosity, a prominent issue highly debated in aluminium welding, was appreciably tackled by the application of interlayer rolling and CMT-PADV technique. Study of weld pool behaviour and weld metal solidification characteristics of heat treatable and non-heat treatable aluminium alloys for thin and thick structures through metallurgical viewpoint can prove to be an important constructive field of study.

Distortion and uneven shrinkage resulting from uncommon solidification behaviour and resulting residual stresses in WAAM structure leaves a wide gap in the knowledge. It will be interesting to insight the stress pattern in open and closed loop structures with varying thicknesses. The maintenance of preheating and interpass temperature and its relation between heat accumulation, residual stress development and mechanical properties is an important area of study. Unweldable aluminium alloys have proven good WAAM capability suggests that there is a necessity to inspect metallurgical aspects of WAAM solidification manner. This fact may lead to requisite of the redefinition of weldability concept or creation of a separate concept of 'WAAMability' of alloys. Also possibility of replacing time consuming interlayer rolling with the single step forming needs to tested to aluminium alloys. Thus, interdependency between weld deposition parameters, microstructure, imperfections and mechanical properties will govern the overall integrity of WAAM of aluminium component and the maturity of WAAM field. Matching mechanical properties of the WAAM product to respective wrought products, no dimensional limitations on product shape, economical advantages, requirement of comparatively less complex and less expensive instruments and simplicity in operation are the prime factors make WAAM incomparable to the techniques such as superplastic forming which were restricted only upto academic interest.

Acknowledgements: This publication was made possible by the sponsorship and support of Lloyd's Register Foundation. The present work was enabled through, and undertaken at, the National Structural Integrity Research Centre (NSIRC), a postgraduate engineering facility for industry-led research into structural integrity establishment and managed by TWI through a network of both national and international Universities. The present review is the author's own work. The author of this paper would like to acknowledge the support from Geoff Melton, Prof. Jonathan Lawrence, Sameehan Joshi, Prof. Stevan Jones and Adrian Addison.

References

1. Ford S, Despeisse M. Additive manufacturing and sustainability: an exploratory study of the advantages and challenges. J Clean Prod. 2016;137:1573–87.

2. Thompson MK, Moroni G, Vaneker T, Fadel G, Campbell RI, Gibson I, et al. Design for Additive Manufacturing: Trends, opportunities, considerations, and constraints. CIRP Ann - Manuf Technol [Internet]. 2016;65(2):737–60. Available from: http://dx.doi.org/10.1016/j.cirp.2016.05.004

3. Labonnote N, Rønnquist A, Manum B, Rüther P. Additive construction: State-of-the-art, challenges and opportunities. Autom Constr [Internet]. 2016;72:347–66. Available from: http://dx.doi.org/10.1016/j.autcon.2016.08.026

4. Gao W, Zhang Y, Ramanujan D, Ramani K, Chen Y, Williams CB, et al. The status, challenges, and future of additive manufacturing in engineering. Comput Des [Internet]. 2015;69:65–89. Available from: http://linkinghub.elsevier.com/retrieve/pii/S0010448515000469

5. Baker R. Method of Making Decorative Articles. US Pat [Internet]. 1920;1–3. Available from: https://drive.google.com/viewerng/viewer?url=patentimages.storage.googleapis.com/pdfs/US1533300.pdf

6. Shockey H. Machine for reclaiming worn brake drums. 1930;1–3.

7. Ujiie A. United States Patent. 1971; Available from: https://www.google.com/patents/US3558846?dq=ujiie+1971&hl=en&sa=X&ei=nmwQVMyECsGzuASw3oHYAw&ved=0CB0Q6AEwAA

8. Ujiie A. Process and apparatus for tripple-electrode MIG welding using short-

circuit and spray-arc deposition. 1972;2–7.

9. K. Kussmaul, F.W. Schoch HL. High quality large components "‘shape welded’" by a SAW process. Vol. 62, Welding Journal. 1983. p. 1983.

10. Dickens PM, Pridham MS, Cobb RC, Gibson I, Dixon MG. Rapid Prototyping Using 3-D Welding. 1960;280–90.

11. Ribeiro F. Metal Based Rapid Prototyping for More Complex Shapes.

12. Zhang YM, Li P, Chen Y, Male AT. Automated system for welding-based rapid prototyping. Mechatronics. 2002;12(1):37–53.

13. Zhang YM, Chen Y, Li P, Male AT. Weld deposition-based rapid prototyping: A preliminary study. J Mater Process Technol. 2003;135(2–3 SPEC.):347–57.

14. Xiong J, Zhang G, Zhang W. Forming appearance analysis in multi-layer single-pass GMAW-based additive manufacturing. Int J Adv Manuf Technol. 2015;80(9–12):1767–76.

15. Xiong J, Yin Z, Zhang W. Forming appearance control of arc striking and extinguishing area in multi-layer single-pass GMAW-based additive manufacturing. Int J Adv Manuf Technol. 2016;87(1–4):579–86.

16. Geng H, Li J, Xiong J, Lin X, Zhang F. Geometric Limitation and Tensile Properties of Wire and Arc Additive Manufacturing 5A06 Aluminum Alloy Parts. J Mater Eng Perform. 2017;26(2):621–9.

17. Ding D, Pan Z, Cuiuri D, Li H. A multi-bead overlapping model for robotic wire and arc additive manufacturing (WAAM). Robot Comput Integr Manuf [Internet]. 2015;31:101–10. Available from: http://dx.doi.org/10.1016/j.rcim.2014.08.008

18. Adebayo a, Mehnen J, Tonnellier X. Limiting Travel Speed in Additive Layer Manufacturing. Trends Weld Res Proc 9th Int Conf. 2013;3:1038–44.

19. Wei PS. Thermal Science of Weld Bead Defects: A Review. J Heat Transfer [Internet]. 2011 Mar 1 [cited 2018 Mar 8];133(3):31005. Available from: http://heattransfer.asmedigitalcollection.asme.org/article.aspx?articleid=1450140

20. Wei PS, Yeh JS, Ting CN, DebRoy T, Chung FK, Lin CL. The effects of Prandtl number on wavy weld boundary. Int J Heat Mass Transf [Internet]. 2009 Jul 1

[cited 2018 Mar 8];52(15–16):3790–8. Available from: https://www.sciencedirect.com/science/article/pii/S0017931009001343

21. Gratzke U, Kapadia PD, Dowden J, Kroos J, Simon G. Theoretical approach to the humping phenomenon in welding processes. J Phys D Appl Phys [Internet]. 1992 Nov 14 [cited 2018 Mar 8];25(11):1640–7. Available from: http://stacks.iop.org/0022-3727/25/i=11/a=012?key=crossref.2125e2c4175f7b36bbd5b804fc1e0ef0

22. Nguyen TC, Weckman DC, Johnson DA, Kerr HW. The humping phenomenon during high speed gas metal arc welding. Sci Technol Weld Join [Internet]. 2005 Jul 4 [cited 2018 Mar 8];10(4):447–59. Available from: http://www.tandfonline.com/doi/full/10.1179/174329305X44134

23. Ding J, Colegrove P, Mehnen J, Ganguly S, Almeida PMS, Wang F, et al. Thermo-mechanical analysis of Wire and Arc Additive Layer Manufacturing process on large multi-layer parts. Comput Mater Sci [Internet]. 2011;50(12):3315–22. Available from: http://dx.doi.org/10.1016/j.commatsci.2011.06.023

24. Somashekara MA, Naveenkumar M, Kumar A, Viswanath C, Simhambhatla S. Investigations into effect of weld-deposition pattern on residual stress evolution for metallic additive manufacturing. Int J Adv Manuf Technol [Internet]. 2017;90(5–8):2009–25. Available from: http://dx.doi.org/10.1007/s00170-016-9510-7

25. Mehnen J, Ding J, Lockett H, Kazanas P. Design forWire and Arc Additive LayerManufacture. Glob Prod Dev [Internet]. 2011;721–7. Available from: http://link.springer.com/10.1007/978-3-642-15973-2

26. Mughal MP, Mufti RA, Fawad H. The mechanical effects of deposition patterns in welding-based layered manufacturing. Proc Inst Mech Eng Part B J Eng Manuf [Internet]. 2007;221(10):1499–509. Available from: http://journals.sagepub.com/doi/10.1243/09544054JEM783

27. Williams SW, Martina F, Addison AC, Ding J, Pardal G, Colegrove P. Wire + Arc Additive Manufacturing. Mater Sci Technol [Internet]. 2016;32(7):641–7. Available from:

http://www.tandfonline.com/doi/full/10.1179/1743284715Y.0000000073

28. Mehnen J, Ding J, Lockett H, Kazanas P. Design study for wire and arc additive manufacture. Int J Prod Dev [Internet]. 2014;19(1/2/3):2. Available from: http://www.scopus.com/inward/record.url?eid=2-s2.0-84898941604&partnerID=tZOtx3y1

29. Venturini G, Montevecchi F, Scippa A, Campatelli G. Optimization of WAAM Deposition Patterns for T-crossing Features. Procedia CIRP [Internet]. 2016;55:95–100. Available from: http://dx.doi.org/10.1016/j.procir.2016.08.043

30. Kazanas P, Deherkar P, Almeida P, Lockett H, Williams S. Fabrication of geometrical features using wire and arc additive manufacture. Proc Inst Mech Eng Part B J Eng Manuf. 2012;226(6):1042–51.

31. Colegrove PA, Martina F, Roy MJ, Szost BA, Terzi S, Williams SW, et al. High Pressure Interpass Rolling of Wire + Arc Additively Manufactured Titanium Components. Adv Mater Res [Internet]. 2014;996:694–700. Available from: http://www.scientific.net/AMR.996.694

32. Szost BA, Terzi S, Martina F, Boisselier D, Prytuliak A, Pirling T, et al. A comparative study of additive manufacturing techniques: Residual stress and microstructural analysis of CLAD and WAAM printed Ti-6Al-4V components. Mater Des. 2016;89:559–67.

33. Martina F, Williams SW, Colegrove P. Improved microstructure and increased mechanical properties of additive manufacture produced Ti-6Al-4V by interpass cold rolling. SFF Symp [Internet]. 2013;490–6. Available from: http://sffsymposium.engr.utexas.edu/Manuscripts/2013/2013-38-Martina.pdf

34. Donoghue J, Antonysamy AA, Martina F, Colegrove PA, Williams SW, Prangnell PB. The effectiveness of combining rolling deformation with Wire-Arc Additive Manufacture on β-grain refinement and texture modification in Ti-6Al-4V. Mater Charact [Internet]. 2016;114:103–14. Available from: http://dx.doi.org/10.1016/j.matchar.2016.02.001

35. Martina F, Colegrove PA, Williams SW, Meyer J. Microstructure of Interpass Rolled Wire + Arc Additive Manufacturing Ti-6Al-4V Components. Metall Mater Trans A Phys Metall Mater Sci. 2015;46(12):6103–18.

36. Adinarayanappa SM, Simhambhatla S. Determination of process parameter for twin-wire weld-deposition based additive manufacturing. In: International design engineering technical conferences. 2016. p. 1–8.

37. Yang D, Wang G, Zhang G. A comparative study of GMAW- and DE-GMAW-based additive manufacturing techniques: thermal behavior of the deposition process for thin-walled parts. Int J Adv Manuf Technol [Internet]. 2017;91(5–8):2175–84. Available from: http://dx.doi.org/10.1007/s00170-016-9898-0

38. Yang D, He C, Zhang G. Forming characteristics of thin-wall steel parts by double electrode GMAW based additive manufacturing. J Mater Process Technol [Internet]. 2016;227:153–60. Available from: http://dx.doi.org/10.1016/j.jmatprotec.2015.08.021

39. Kou S. Metallurgy Second Edition Welding Metallurgy [Internet]. Vol. 822, Wiley. 2003. 466 p. Available from: http://books.google.com/books?hl=en&lr=&id=N8gICBzzgRwC&oi=fnd&pg=PR7&dq=WELDING+METALLURGY&ots=KbMCYOBY2l&sig=bUKTMZRhqD6LE6kzQIivLlTfJK4

40. Somashekara MA, Suryakumar S. Studies on Dissimilar Twin-Wire Weld-Deposition for Additive Manufacturing Applications. Trans Indian Inst Met. 2017;70(8):2123–35.

41. Qi Z, Cong B, Qi B, Sun H, Zhao G, Ding J. Microstructure and mechanical properties of double-wire + arc additively manufactured Al-Cu-Mg alloys. J Mater Process Technol [Internet]. 2018;255:347–53. Available from: http://dx.doi.org/10.1016/j.jmatprotec.2017.12.019

42. Martina F, Williams S. Wire + arc additive manufacturing vs . traditional machining from solid: a cost comparisonfrom solid : 2015;

43. Gu D. Laser Additive Manufacturing (AM): Classification, Processing Philosophy, and Metallurgical Mechanisms [Internet]. Laser Additive Manufacturing of High-Performance Materials. 2015. 15-71 p. Available from: http://link.springer.com/10.1007/978-3-662-46089-4_2

44. Herzog D, Seyda V, Wycisk E, Emmelmann C. Additive manufacturing of metals. Acta Mater [Internet]. 2016;117:371–92. Available from:

http://dx.doi.org/10.1016/j.actamat.2016.07.019

45. Xiong J, Zhang G. Online measurement of bead geometry in GMAW-based additive manufacturing using passive vision. Meas Sci Technol. 2013;24(11).

46. Geng H, Li J, Xiong J, Lin X, Zhang F. Optimization of wire feed for GTAW based additive manufacturing. J Mater Process Technol [Internet]. 2017;243:40–7. Available from: http://dx.doi.org/10.1016/j.jmatprotec.2016.11.027

47. Withers PJ, Bhadeshia HKDH. Residual stress. Part 1 – Measurement techniques. Mater Sci Technol [Internet]. 2001 Apr 19 [cited 2018 Mar 8];17(4):355–65. Available from: http://www.tandfonline.com/doi/full/10.1179/026708301101509980

48. Withers PJ, Bhadeshia HKDH. Residual stress. Part 2 – Nature and origins. Mater Sci Technol [Internet]. 2001 Apr 19 [cited 2018 Mar 8];17(4):366–75. Available from: http://www.tandfonline.com/doi/full/10.1179/026708301101510087

49. Wang P, Hu S, Shen J, Liang Y. Characterization the contribution and limitation of the characteristic processing parameters in cold metal transfer deposition of an Al alloy. J Mater Process Technol [Internet]. 2017;245:122–33. Available from: http://dx.doi.org/10.1016/j.jmatprotec.2017.02.019

50. Cong B, Ouyang R, Qi B, Ding J. Influence of Cold Metal Transfer Process and Its Heat Input on Weld Bead Geometry and Porosity of Aluminum-Copper Alloy Welds. Rare Met Mater Eng [Internet]. 2016;45(3):606–11. Available from: http://linkinghub.elsevier.com/retrieve/pii/S1875537216300807

51. Gu J, Ding J, Williams SW, Gu H, Ma P, Zhai Y. The effect of inter-layer cold working and post-deposition heat treatment on porosity in additively manufactured aluminum alloys. J Mater Process Technol. 2016;230:26–34.

52. Cong B, Qi Z, Qi B, Sun H, Zhao G, Ding J. A Comparative Study of Additively Manufactured Thin Wall and Block Structure with Al-6.3%Cu Alloy Using Cold Metal Transfer Process. Appl Sci [Internet]. 2017;7(3):275. Available from: http://www.mdpi.com/2076-3417/7/3/275

53. Consonni M. The 2017 edition of BS EN ISO 15614-1: review of the changes and their practical implications. Cambridge, UK; 2018.

54. Melfi T. ASME IX Heat input code changes. In: EPRI Conference. 2010.

55. Pickin CG, Young K. Evaluation of cold metal transfer (CMT) process for welding aluminium alloy. Sci Technol Weld Join [Internet]. 2006;11(5):583–5. Available from: http://www.tandfonline.com/doi/full/10.1179/174329306X120886

56. Pickin CG, Williams SW, Lunt M. Characterisation of the cold metal transfer (CMT) process and its application for low dilution cladding. J Mater Process Technol [Internet]. 2011;211(3):496–502. Available from: http://dx.doi.org/10.1016/j.jmatprotec.2010.11.005

57. Kumar NP, Arungalai Vendan S, Siva Shanmugam N. Investigations on the parametric effects of cold metal transfer process on the microstructural aspects in AA6061. J Alloys Compd [Internet]. 2016;658:255–64. Available from: http://dx.doi.org/10.1016/j.jallcom.2015.10.166

58. Ola OT, Doern FE. A study of cold metal transfer clads in nickel-base INCONEL 718 superalloy. Mater Des [Internet]. 2014;57:51–9. Available from: http://dx.doi.org/10.1016/j.matdes.2013.12.060

59. Elrefaey A. Effectiveness of cold metal transfer process for welding 7075 aluminium alloys. Sci Technol Weld Join [Internet]. 2015;20(4):280–5. Available from: http://www.tandfonline.com/doi/full/10.1179/1362171815Y.0000000017

60. Gungor B, Kaluc E, Taban E, SIK Ş.Ş A. Mechanical and microstructural properties of robotic Cold Metal Transfer (CMT) welded 5083-H111 and 6082-T651 aluminum alloys. Mater Des [Internet]. 2014;54:207–11. Available from: http://dx.doi.org/10.1016/j.matdes.2013.08.018

61. Wang H, Jiang W, Ouyang J, Kovacevic R. Rapid prototyping of 4043 Al-alloy parts by VP-GTAW. J Mater Process Technol. 2004;148(1):93–102.

62. Cong B, Ding J, Williams S. Effect of arc mode in cold metal transfer process on porosity of additively manufactured Al-6.3%Cu alloy. Int J Adv Manuf Technol. 2014;76(9–12):1593–606.

63. Gu J, Ding J, Williams SW, Gu H, Bai J, Zhai Y, et al. The strengthening effect of inter-layer cold working and post-deposition heat treatment on the additively manufactured Al-6.3Cu alloy. Mater Sci Eng A [Internet]. 2016;651:18–26.

Available from: http://dx.doi.org/10.1016/j.msea.2015.10.101

64. Gu J, Wang X, Bai J, Ding J, Williams S, Zhai Y, et al. Deformation microstructures and strengthening mechanisms for the wire+arc additively manufactured Al-Mg4.5Mn alloy with inter-layer rolling. Mater Sci Eng A [Internet]. 2018;712(August 2017):292–301. Available from: https://doi.org/10.1016/j.msea.2017.11.113

65. Gu J, Cong B, Ding J, Williams SW, Zhai Y. Wire+Arc Additive Manufacturing of Aluminium. SFF Symp Austin Texas. 2014;451–8.

66. Ding Y, Muñiz-Lerma JA, Trask M, Chou S, Walker A, Brochu M. Microstructure and mechanical property considerations in additive manufacturing of aluminum alloys. MRS Bull. 2016;41(10):745–51.

67. Fixter J, Gu J, Ding J, Williams SW, Prangnell PB. Preliminary Investigation into the Suitability of 2xxx Alloys for Wire-Arc Additive Manufacturing. Mater Sci Forum [Internet]. 2016;877:611–6. Available from: http://www.scientific.net/MSF.877.611

68. Silva CMA, Bragança IMF, Cabrita A, Quintino L, Martins PAF. Formability of a wire arc deposited aluminium alloy. J Brazilian Soc Mech Sci Eng. 2017;39(10):4059–68.

69. Ding D, Pan Z, Cuiuri D, Li H. A tool-path generation strategy for wire and arc additive manufacturing. Int J Adv Manuf Technol. 2014;73(1–4):173–83.

70. Newman ST, Zhu Z, Dhokia V, Shokrani A. Process planning for additive and subtractive manufacturing technologies. CIRP Ann - Manuf Technol [Internet]. 2015;64(1):467–70. Available from: http://dx.doi.org/10.1016/j.cirp.2015.04.109

71. Ding D, Pan Z, Cuiuri D, Li H, Larkin N. Adaptive path planning for wire-feed additive manufacturing using medial axis transformation. J Clean Prod [Internet]. 2016;133(June):942–52. Available from: http://dx.doi.org/10.1016/j.jclepro.2016.06.036

72. Song Y-A, Park S, Chae S-W. 3D welding and milling: part II—optimization of the 3D welding process using an experimental design approach. Int J Mach Tools Manuf [Internet]. 2005;45(9):1063–9. Available from: http://linkinghub.elsevier.com/retrieve/pii/S0890695504003086

73. Li F, Chen S, Shi J, Tian H, Zhao Y. Evaluation and Optimization of a Hybrid Manufacturing Process Combining Wire Arc Additive Manufacturing with Milling for the Fabrication of Stiffened Panels. Appl Sci [Internet]. 2017;7(12):1233. Available from: http://www.mdpi.com/2076-3417/7/12/1233

74. Prado-Cerqueira JL, Diéguez JL, Camacho AM. Preliminary development of a Wire and Arc Additive Manufacturing system (WAAM). Procedia Manuf [Internet]. 2017;13:895–902. Available from: https://doi.org/10.1016/j.promfg.2017.09.154

75. Colegrove PA, Donoghue J, Martina F, Gu J, Prangnell P, Hönnige J. Application of bulk deformation methods for microstructural and material property improvement and residual stress and distortion control in additively manufactured components. Scr Mater [Internet]. 2017;135(November):111–8. Available from: http://dx.doi.org/10.1016/j.scriptamat.2016.10.031

76. Xiong J, Zhang G. Adaptive control of deposited height in GMAW-based layer additive manufacturing. J Mater Process Technol [Internet]. 2014;214(4):962–8. Available from: http://dx.doi.org/10.1016/j.jmatprotec.2013.11.014

77. Xiong J, Lei Y, Chen H, Zhang G. Fabrication of inclined thin-walled parts in multi-layer single-pass GMAW-based additive manufacturing with flat position deposition. J Mater Process Technol [Internet]. 2017;240(May 2017):397–403. Available from: http://dx.doi.org/10.1016/j.jmatprotec.2016.10.019

78. Colegrove PA, Coules HE, Fairman J, Martina F, Kashoob T, Mamash H, et al. Microstructure and residual stress improvement in wire and arc additively manufactured parts through high-pressure rolling. J Mater Process Technol [Internet]. 2013;213(10):1782–91. Available from: http://dx.doi.org/10.1016/j.jmatprotec.2013.04.012

79. Filomeno Martina, Matthew Roy, Paul Colegrove SWW. Residual Stress Reduction in High Pressure Interpass Rolled. Solid Free Fabr Proc. 2014;(August):89–94.

80. Honnige J, Williams S, Roy M, Colegrove P, Ganguly S. Residual Stress Characterization and Control in the Additive Manufacture of Large Scale Metal Structures. In: Material reseach proceedings [Internet]. 2016. p. 455–60.

Available from: http://www.mrforum.com/product/9781945291173-77

81. Almeida P, Williams S. Innovative process model of Ti–6Al–4V additive layer manufacturing using cold metal transfer (CMT). Solid Free Fabr Symp. 2010;(June):25–36.

82. Wagiman A, Bin Wahab MS, Mohid Z, Mamat A. Effect of GMAW-CMT Heat Input on Weld Bead Profile Geometry for Freeform Fabrication of Aluminium Parts. Appl Mech Mater [Internet]. 2013;465–466:1370–4. Available from: http://www.scientific.net/AMM.465-466.1370

83. Zhang C, Li Y, Gao M, Zeng X. Wire arc additive manufacturing of Al-6Mg alloy using variable polarity cold metal transfer arc as power source. Mater Sci Eng A [Internet]. 2018;711(November 2017):415–23. Available from: https://doi.org/10.1016/j.msea.2017.11.084

84. Wang F, Williams S, Colegrove P, Antonysamy AA. Microstructure and Mechanical Properties of Wire and Arc Additive Manufactured Ti-6Al-4V. Metall Mater Trans A [Internet]. 2013 Feb 28 [cited 2018 Mar 1];44(2):968–77. Available from: http://link.springer.com/10.1007/s11661-012-1444-6

85. Zhang J, Wang X, Paddea S, Zhang X. Fatigue crack propagation behaviour in wire+arc additive manufactured Ti-6Al-4V: Effects of microstructure and residual stress. Mater Des [Internet]. 2016;90:551–61. Available from: http://dx.doi.org/10.1016/j.matdes.2015.10.141

86. Zhang J, Zhang X, Wang X, Ding J, Traoré Y, Paddea S, et al. Crack path selection at the interface of wrought and wire + arc additive manufactured Ti–6Al–4V. Mater Des [Internet]. 2016 Aug 15 [cited 2018 Mar 1];104:365–75. Available from: https://www.sciencedirect.com/science/article/pii/S0264127516306293

87. Zhang X, Martina F, Ding J, Wang X, Williams S. Fracture toughness and fatigue crack growth rate properties in wire + arc additive manufactured Ti-6Al-4V. Fatigue Fract Eng Mater Struct [Internet]. 2017 May 1 [cited 2018 Mar 1];40(5):790–803. Available from: http://doi.wiley.com/10.1111/ffe.12547

88. Moore P, Addison AC, M. N. Mechanical Performance of Wire Plus Arc Additive Manufactured Steel and Stainless Steel Structures(Paper). In: THE

FIRST INTERNATIONAL CONGRESS ON WELDING, ADDITIVE MANUFACTURING AND ASSOCIATED NON DESTRUCTIVE TESTING, ICWAM 2017. 2017.

89. Fu Y, Zhang H, Wang G, Wang H. Investigation of mechanical properties for hybrid deposition and micro-rolling of bainite steel. J Mater Process Technol [Internet]. 2017;250(February):220–7. Available from: http://dx.doi.org/10.1016/j.jmatprotec.2017.07.023

90. Kotecki D, Armao F. Stainless steels properties - how to weld them where to use them. The Lincoln electric company; 2003.

91. Ji L, Lu J, Liu C, Jing C, Fan H, Ma S. Microstructure and mechanical properties of 304L steel fabricated by arc additive manufacturing. Wang Y, editor. MATEC Web Conf [Internet]. 2017 Oct 25 [cited 2018 Mar 2];128:3006. Available from: http://www.matec-conferences.org/10.1051/matecconf/201712803006

92. Metals Handbook (Vol.2) - Properties and Selection: Nonferrous alloys and Special-purpose materials. 10th ed. ASM International; 1990.

93. TWI-global [Internet]. [cited 2018 Jan 22]. Available from: https://www.twi-global.com/technical-knowledge/best-practiceguides/%0Aarc-welding-aluminium-section-2-process-and-consumables-selection/

94. Xu W, Gottos M, Roe M, Wood M, Wilson M. Impact tests on welded joints in 6000 series aluminium alloy extrusion for rail vehicles. 2008.

95. Nobel P. Method and apparatus for electric arc welding. 1919;

96. Carpenter O, Kerr H. Method and apparatus for metal coating metal pipes by electric fusion. 1943;1–10.

97. White W. Pressure roller and method of manufacture. 1962;2–5.

98. Brandi H, Luckow H. Method of making large structural one-piece parts of metal, particularly one-piece shafts. 1974;1–8.

99. Hitoshi T. Production of powder of metal or nonmetal or alloy thereof. 1984;59129702(c):5–6.

100. Ayres P, Edmonds D, Hartwig D, Merker D, Weber C. Method and apparatus for controlling weld bead shape to eliminate microfissure defects when shape

melting austenitic materials. 1987;1–10.

101. Doyle T, Ryan P. Method and apparatus for automatic vapor cooling when shape melting a component. 1988;1–7.

102. Muscato G, Spampinato G, Cantelli L. A closed loop welding controller for a rapid manufacturing process. IEEE Int Conf Emerg Technol Fact Autom ETFA. 2008;1080–3.

103. Irving R. An electroslag welded vessel. Iron Age. 1970;205.

104. Wiktorowicz R, Melton G. Shielding gas selection for controlled dip transfer (short arc) welding. TWI Bull.

Table 1 Hot short composition range for aluminium binary system

Alloy system	**Hot short composition range (wt. %)**
Al-Si	0.5 – 1.2
Al-Cu	2.0 – 4.0
Al-Mn	1.5 – 2.5
Al-Mg	0.5 – 2.5
Al-Zn	4.0 – 5.0
Al-Fe	1.0 – 1.5

Table 2 Major areas of study of WAAM technique in recent past

Area of study	Year	Specific area of study	Material / Filler wire	Studied by
Design	2011	• Cross structures • Root path determination	Steel	Mehnen et al. (25)
		• Inclined wall preparation • Preparation of horizontal wall and closed shape	Steel (ER70S-6), Aluminium (4043)	Kazanas et al. (30)
	2014	• Deposition patterns • Cross structures	Mild steel, Titanium (Ti-6Al-4V)	Mehnen et al. (28)
		• Tool path planning	Mild steel	Ding et al. (69)
	2015	• Hybrid manufacturing	-	Newman et al. (70)
	2016	• T-crossing	Steel (ER70S-6)	Venturini et al. (29)
		• Adaptive path generation	Steel	Ding et al. (71)
Process variation	2005	• Hybrid manufacturing using milling	Steel (ER70S-6)	Song et al. (72)
	2014	• Twin wire GMAW	Steel (ER70S-6) & Steel ER110S-6	Adinarayanappa and Simhambhatla (36)
	2016	• Double electrode GMAW	Steel (H08Mn2Si)	Yang et al. (37)
		• Dissimilar twin wire deposition (functionally gradient part formation)	Steel (ER70S-6) & Steel ER110S-G	Somashekara and Suryakumar (40)

		• Double electrode GMAW	Steel (H08Mn2Si)	Yang et al. (38)
	2017	• Hybrid manufacturing with milling	Aluminium 2325	Li et al. (73)
		• Hybrid manufacturing	Steel (ER70S-6)	Prado-Cerqueira et al. (74)
	2018	• Dissimilar twin wire GTAW deposition	Aluminium ER2319 and ER5087	Qi et al. (41)
Residual stress	2007	• Finite elemental structural study	Steel (Simulation)	Mughal et al. (26)
	2011	• Computer simulation	Steel	Ding et al. (23)
	2015	• Distortion control	Steel, Aluminium and Titanium (Ti-6Al-4V)	Williams et al. (27)
	2016	• Computational model for twin wire AM	Steel (ER70S-6)	Somashekara et al. (24)
		• Bulk deformation	Steel (ER70S-6)	Colegrove et al. (75)
		• Microstructure	Titanium (Ti-6Al-4V)	Szost et al. (32)
Forming appeara-nce	2014	• Passive vision sensor system	Steel	Xiong and Zhang (76)
	2015	• Parametric study	Steel	Xiong et al. (14)
		• Bead overlapping factor	Steel	Ding et al. (17)
	2016	• Double electrode GMAW parametric study	Steel (H08Mn2Si)	Yang et al. (38)
		• Minimum angle and curvature of radius	Aluminium 5A06	Geng et al. (16)

		• Control of arc start and end	Steel	Xiong et al. (15)
	2017	• Inclined wall structure	Steel (H08Mn2Si)	Xiong et al. (77)
Interlayer-rolling and its effect on microstru-cture, mechani-cal properties and residual stresses	2013	• Effect of different profiled rollers	Steel (ER70S-6)	Colegrove et al. (78)
		• Grain structure refining • Mechanical properties	Titanium (Ti-6Al-4V)	Martina et al. (33)
	2014	• Distortion • Refined microstructure	Titanium (Ti-6Al-4V)	Colegrove et al.(31)
		• Reduction of residual stresses	Titanium (Ti-6Al-4V)	Martina et al. (79)
	2016	• Controlling residual stresses	Titanium (Ti-6Al-4V)	Honnige et al. (80)
		• Precipitation hardenable alloy	Aluminium (ER2319)	Gu et al. (63)
		• Porosity formation behaviour in work and precipitation hardenable alloy	Aluminium (ER2319 and 5087)	Gu et al. (51)
		• β grain refinement in Ti-6Al-4V	Titanium (Ti-6Al-4V)	Donoghue et al. (34)
	2017	• Al-Mg4.5Mn alloy	Aluminium (ER5087)	Gu et al. (64)
Cold metal transfer (CMT)	2010	• Application for Ti-6Al-4V	Titanium (Ti-6Al-4V)	Almeida and Williams (81)
	2014	• Parametric study with AlSi5	Aluminium (AlSi5)	Wagiman et al. (82)
		• Variants of CMT technique • Effect on porosity	Aluminium (2319)	Cong et al. (62)
	2016	• Variants of CMT technique	Aluminium (ER2319)	Cong et al. (50)

	2017	• Wall and block structure	Aluminium (ER2319)	Cong et al. (52)
	2018	• Varying polarity and microstructural considerations	Al-6Mg	Zhang et al. (83)
Fatigue failure and toughness	2013	• Fatigue life	Titanium (Ti-6Al-4V)	Wang et al. (84)
	2016	• Fatigue crack growth propagation	Titanium (Ti-6Al-4V)	Zhang et al. (85)
		• Fatigue crack path selection	Titanium (Ti-6Al-4V)	Zhang et al. (86)
	2017	• Fatigue crack growth rate	Titanium (Ti-6Al-4V)	Zhang et al. (87)

Table 3 Comparison of tensile properties of WAAM parts (vertical direction / longitudinal to build direction) with comparable wrought / filler wire

Alloy	Wrought product / filler wire			WAAM product			Reported by
	Yield strength (MPa)	**Ultimate tensile strength (MPa)**	**Elong-ation (%)**	**Yield strength (MPa)**	**Ultimate tensile strength (MPa)**	**Elong-ation (%)**	
Titanium (Ti-6Al-4V)	950	1030	11	870	920	12	Martina et al.(33)
Steel (ER70S)	448	480	22	402 (max)	-	-	Moore et al. (88)
Stainless Steel (316L)	452	520	30	422 (max)	-	-	
Bainitic steel	1230	-	11	1010	-	6	Fu et al. (89)
Stainless steel (304)	552	241	55	235	678	55.6	Kotecki and Armao (90) and Ji et al. (91)

Table 4 Comparison of conventional dip transfer (CDT) and CMT mode based on operation cycle

Stage	**CDT**		**CMT**		
	Current	Voltage	Current	Voltage	Wire feed
Arc burning	LD	SD	LI	SI	Feed
Arc collapse	SI	LD	LD	SD	Feed
Short circuiting	LI	SI	SI	LD	Feed
Arc re-ignition	SD	LI	LI	LI	Retract

*LI – Large increase, LD – Large decrease, SI – Small increase, SD – Small decrease

Table 5 Effect of different metal deposition conditions and different loads of inter-layer rolling on porosity in aluminium alloys

Filler wire	Condition	Mode of metal transfer	Pore count	Pore diameter	Length/area of consideration for pore count	Reported by
2319	AD	CMT	155	10-50µm	15mm length	Cong et al.(62)
			42	50-100µm		
			25	> 100µm		
		CMTP	21	10-50µm		
			7	50-100µm		
			0	> 100µm		
		CMTADV	17	10-50µm		
			0	> 50 µm		
		CMTPADV	0	> 10µm		
	AD	CMTPADV	614	13.5µm	120mm^2	Gu et al. (51)
	R15		192	12.5µm		
	R30		5	8.8µm		
	HT		2001	15.5µm		
	AD block structure	CMTP	180	15µm	225mm^2	Cong et al. (52)
			40	25µm		
			15	35µm		
	AD wall structure		110	15µm		
			50	25µm		
			100	35µm		
			134	> 35µm		
	AD block structure	CMTADV	60	15µm		
			35	25µm		
			11	35µm		
	AD wall structure		120	15µm		
			90	25µm		
			30	35µm		
			85	> 35µm		
5087	AD	CMTP	454	25.1µm	120mm^2	Gu et al. (51)
	R15		336	33.2µm		
	R30		11	13µm		
	HT		359	9.6µm		

*AD – As deposited, R15 – Rolled 15kN, R30 – Rolled 30kN, HT – Heat treated

Table 6 Tensile properties of different aluminium alloys based on different testing conditions

Filler wire	Condition	YS (MPa)	UTS (MPa)	Percentage Elongation	Reported by
5087	As deposited	142	291	22.4	Gu et al. (64)
	Rolled 15kN	169	320	35	
	Rolled 30kN	149	311	39	
	Rolled 45kN	200	344	47	
	Wrought (5083-O)	145	290	22	ASM Vol.2 (92)
2024	As deposited	175	290	12	Fixter et al. (67)
	Rolled 45kN	315	375	8	
	T4	335	465	15	
	T6	415	505	8	
	Rolled 45kN + T6	415	500	11	
	Wrought (2024-T62)	345	440	5	ASM Vol.2 (92)
2319	As deposited	130	260	15	Gu et al. (63)
	Rolled 15kN	140	270	14.5	
	Rolled 30kN	185	285	11	
	Rolled 45kN	245	315	9	
	T6	315	465	13	
	Rolled 45kN + T6	310	460	16	
	Wrought (2219-T62)	220	340	7	ASM Vol.2 (92)
2319	Vertical	106	258	15.5	Gu et al. (65)
	Horizontal	114	263	18.3	
Al-6Mg	CMT	-	320	-	Zhang et al. (83)
	CMTP	-	285	-	
	VP-CMT	-	325	-	

*VPCMT – Varying polarity cold metal transfer mode

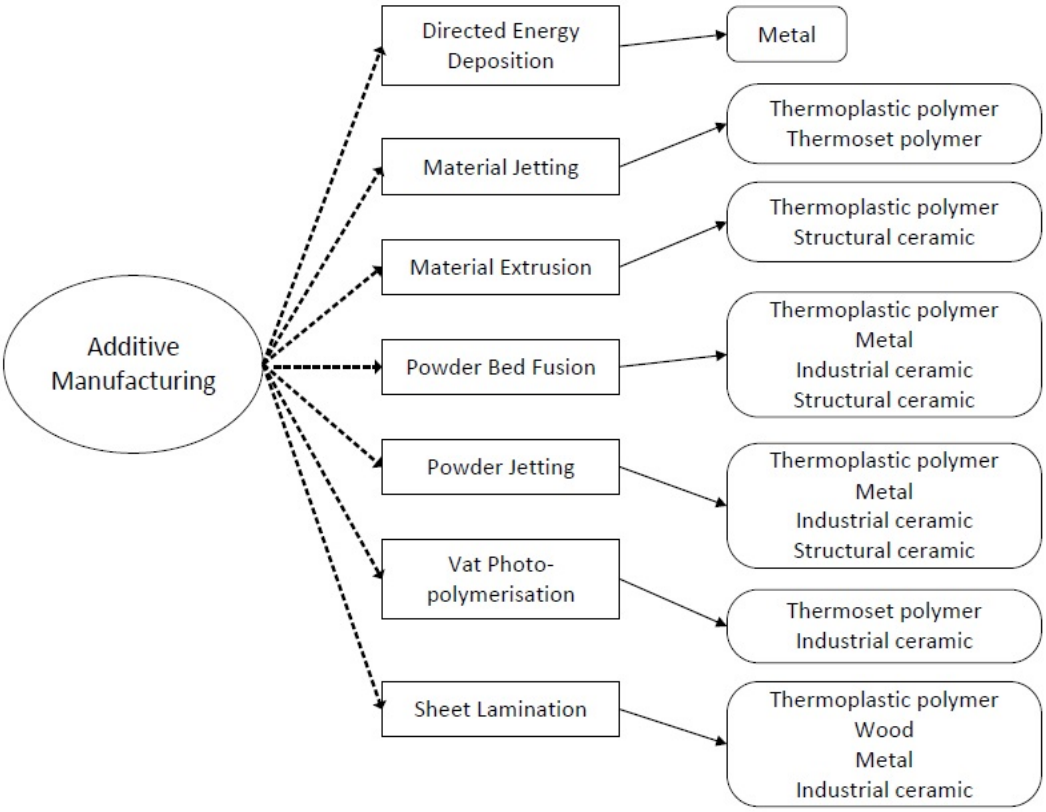

Figure 1 Classification of AM processes with respective material handling capabilities

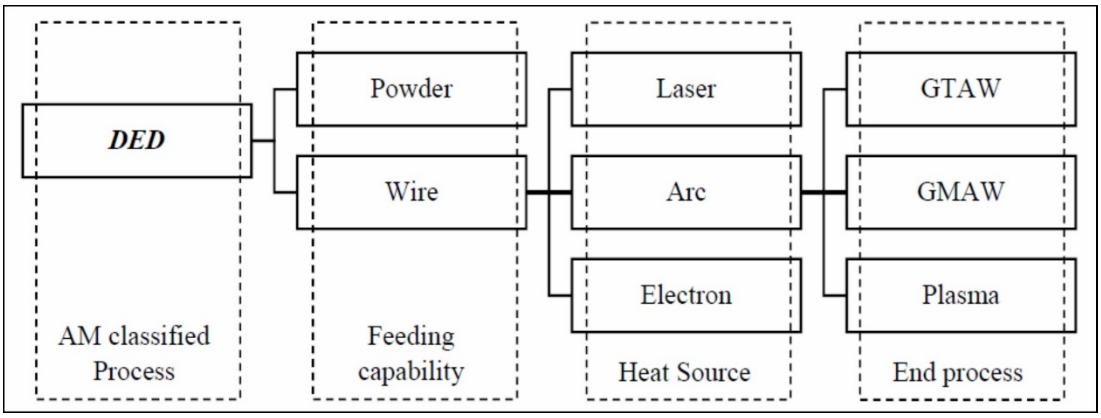

Figure 2 Typical classification of WAAM

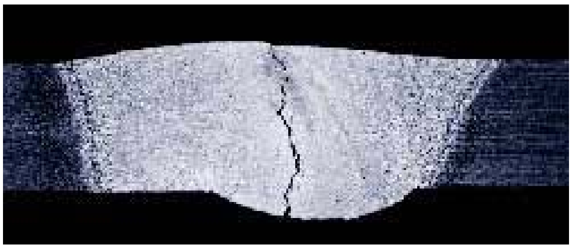

Figure 3 Solidification cracking in aluminium welding (93)

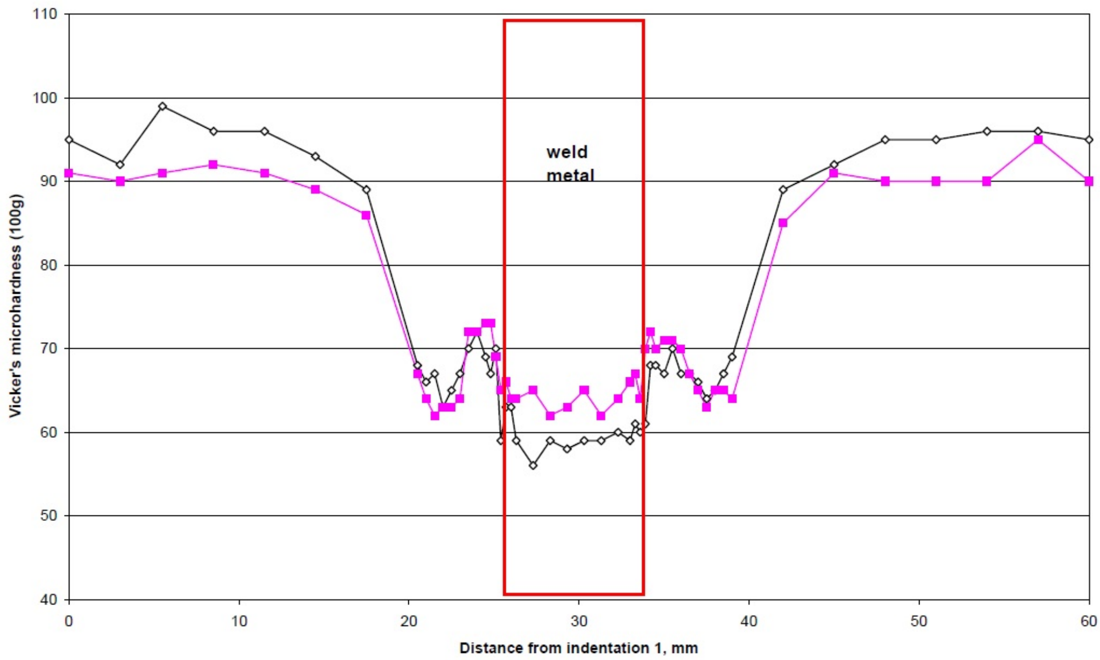

Figure 4 Microhardness variation in the 6xxx series alloy across the weld when welded by MIG/MAG (94)

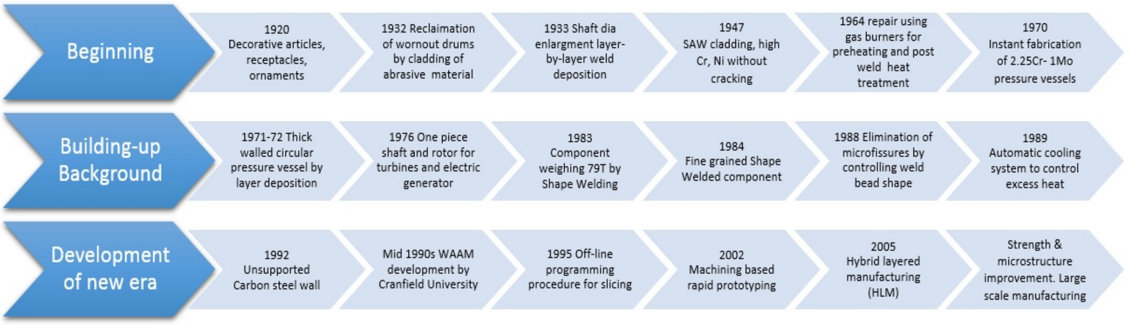

Figure 5 History of WAAM (5–12,31,33–35,72,95–103)

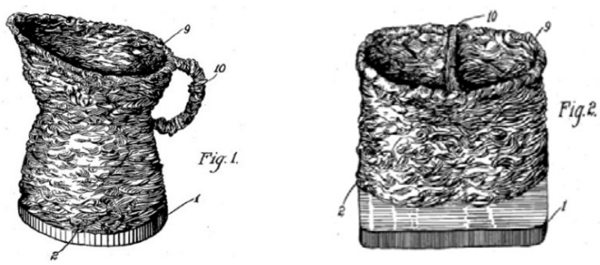

Figure 6 Schematic diagram showing superposed deposit of metal (5)

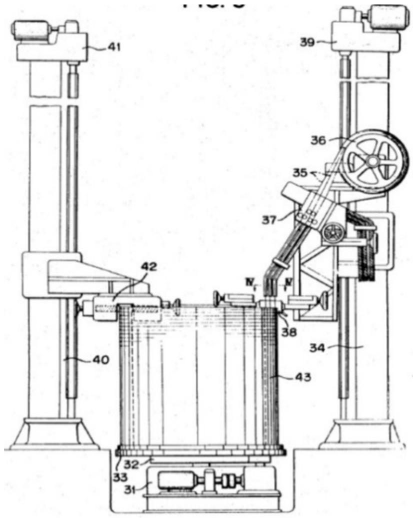

Figure 7 Technical drawing showing a thick walled circular cross-section pressure vessel (7)

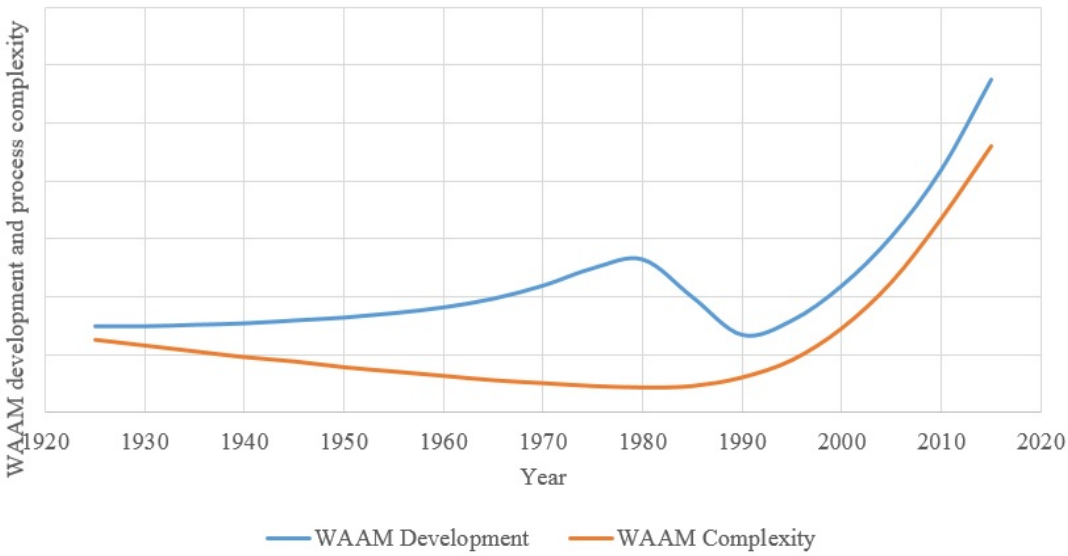

Figure 8 Development and complexity of WAAM process over the years

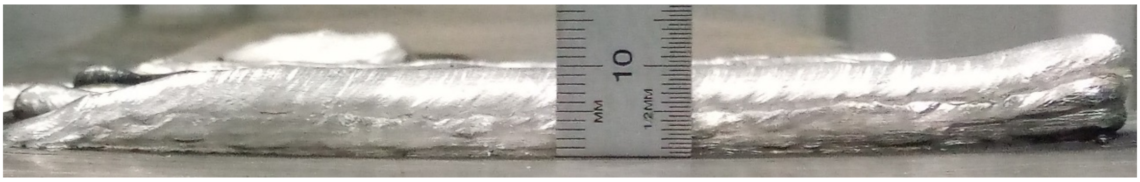

Figure 9 Single bead multi-layer WAAM part without start and end control

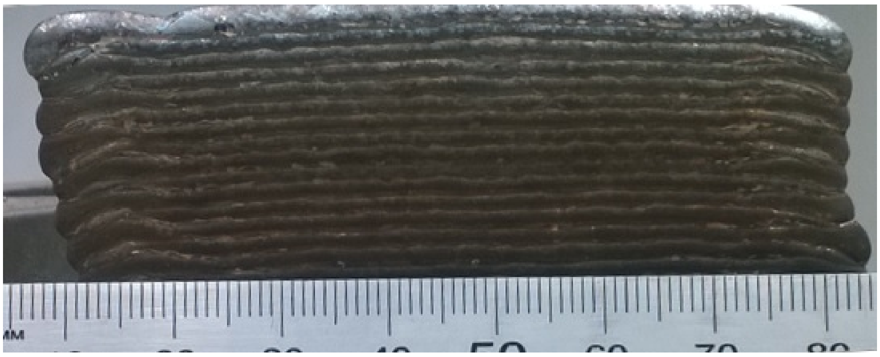

Figure 10 Single bead multi-layer WAAM part with controlled start and end

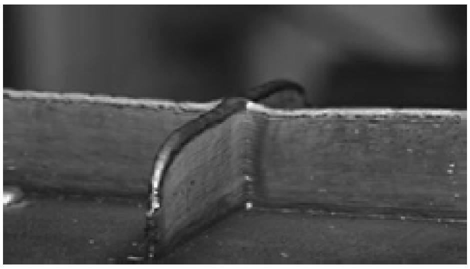

Figure 11 Deposition of cross structure(25)

Figure 12 Horizontal features deposition without support(27)

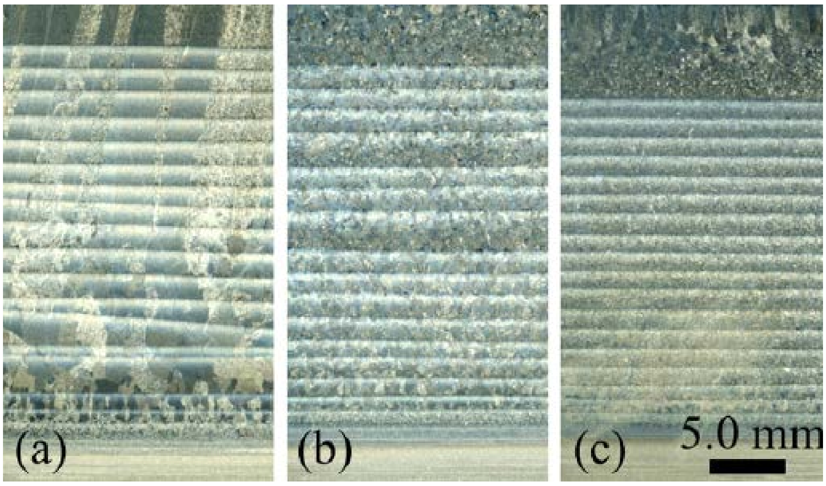

Figure 13 Macrostructural comparison of grain size variation in different load application condition;(a) without loading, (b) load of 50kN and (c) load of 75kN (34)

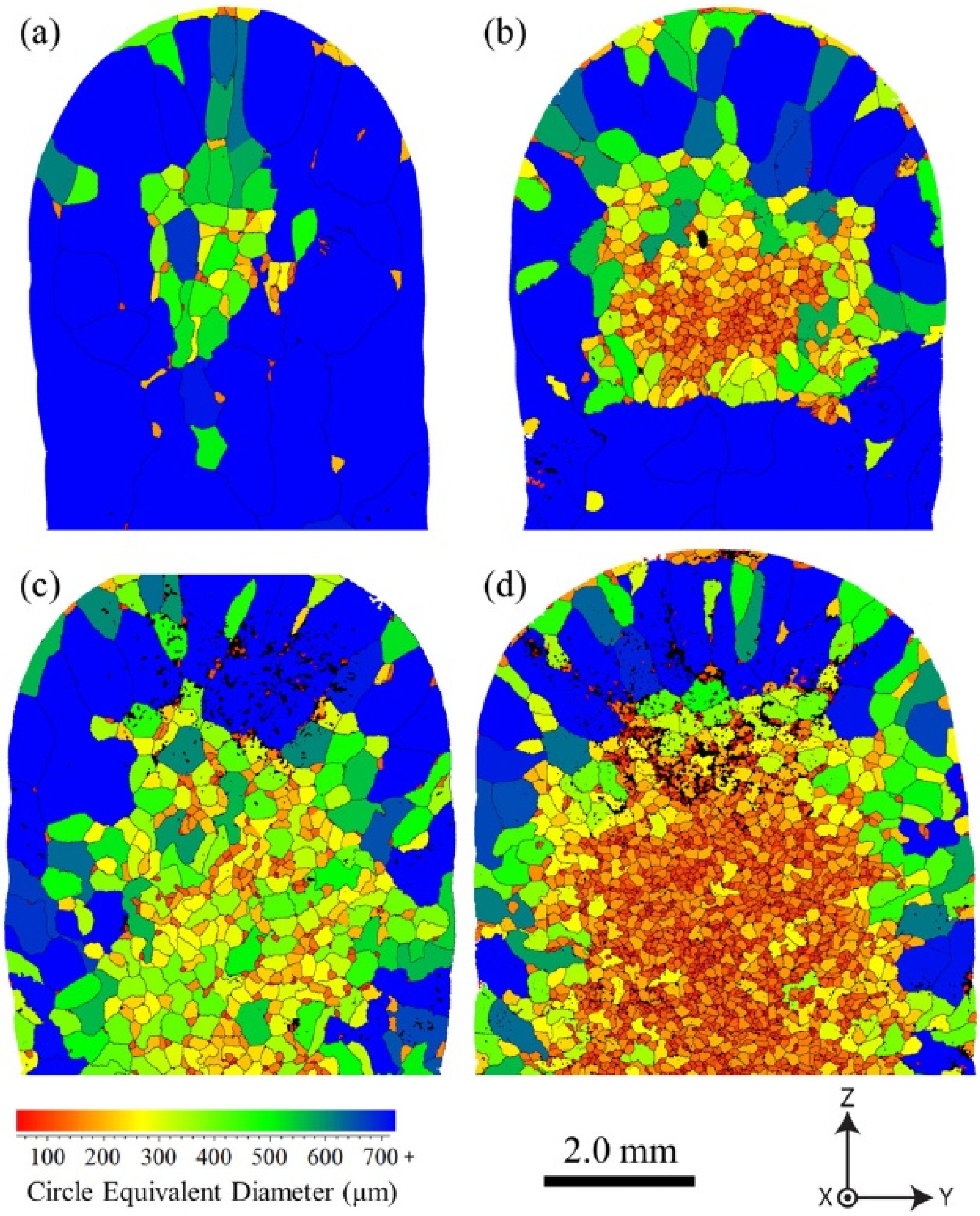

Figure 14 EBSD map of effect of rolling on beta grain size; (a) and (b) with application load to the second last layer only and (c) and (d) rolling applied to the each layer, for both conditions rolling laods 50kN and 75kN respectively

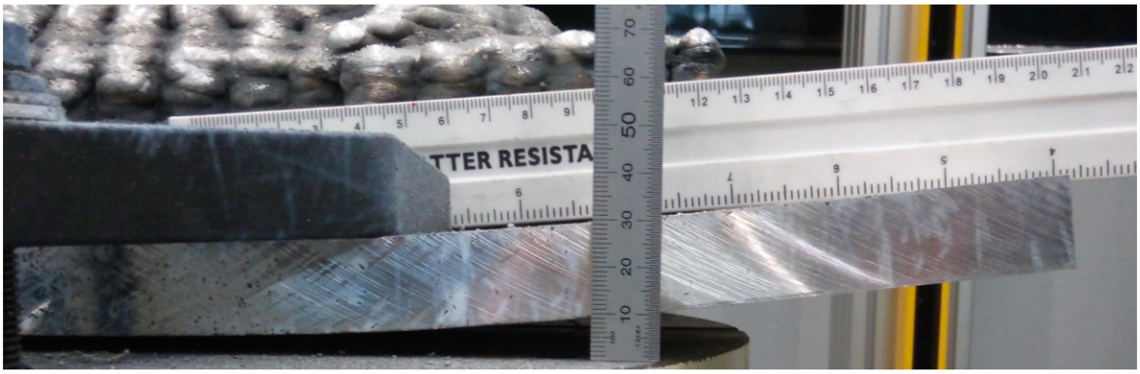

Figure 15 Large distortion produced due to multiple thermal cycles during production of WAAM object

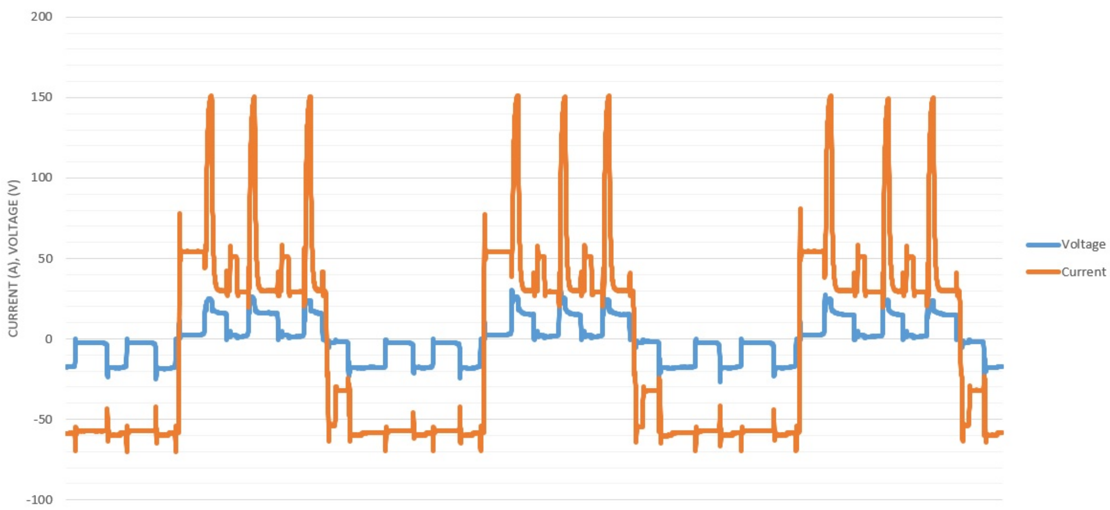

Figure 16 Current and voltage waveforms of CMT process

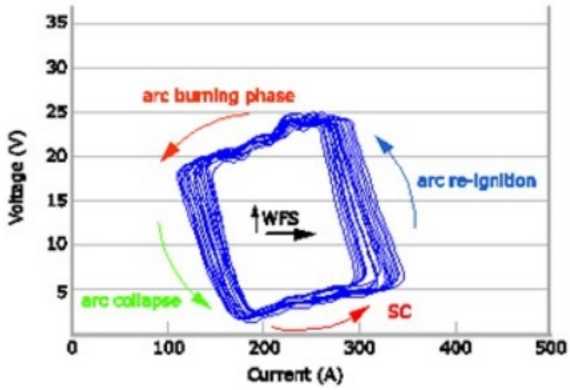

Figure 17 Cyclogram of current and voltage variation for conventional dip transfer (104)

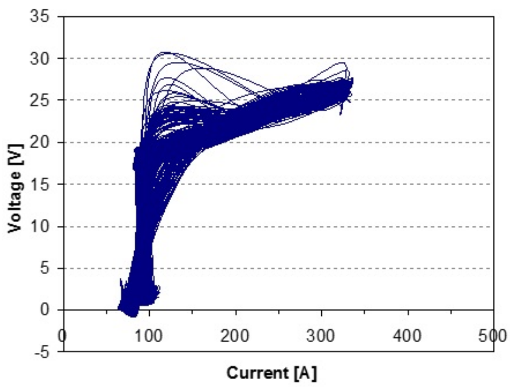

Figure 18 Cyclogram of current and voltage variation for CMT transfer mode (Private communication with Melton, Jan 2018)

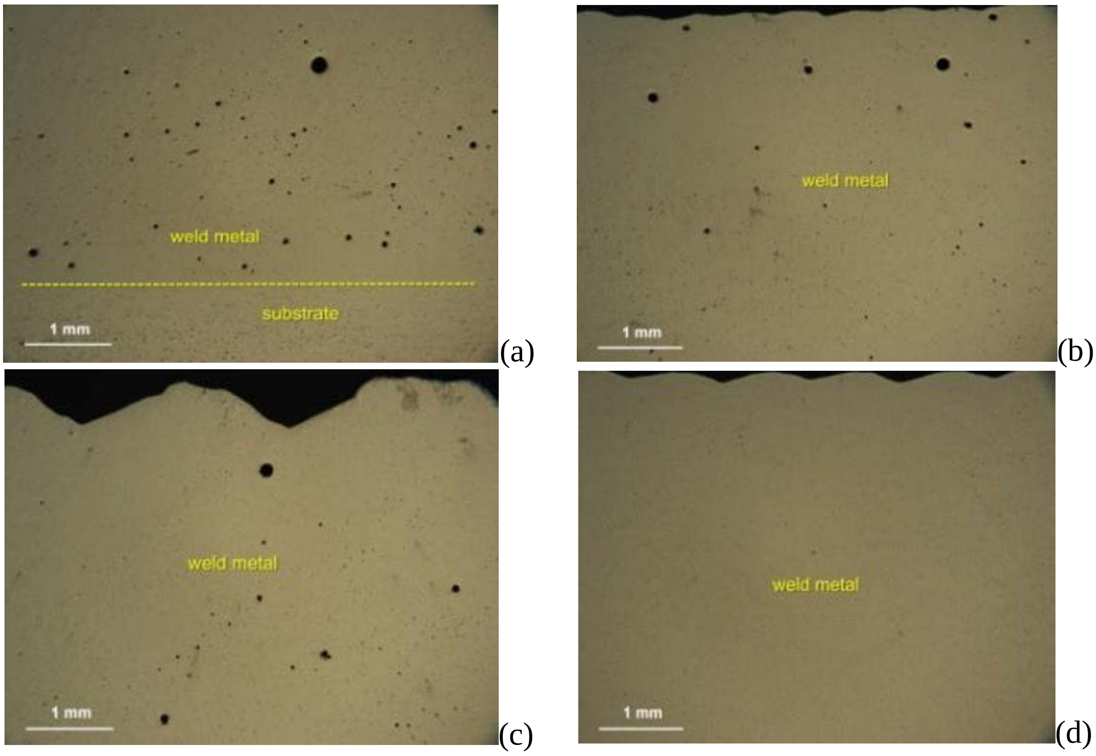

Figure 19 Porosity distribution in (a) Conventional CMT (b) CMT-P (c) CMT-ADV and (d) CMT-PADV(50)

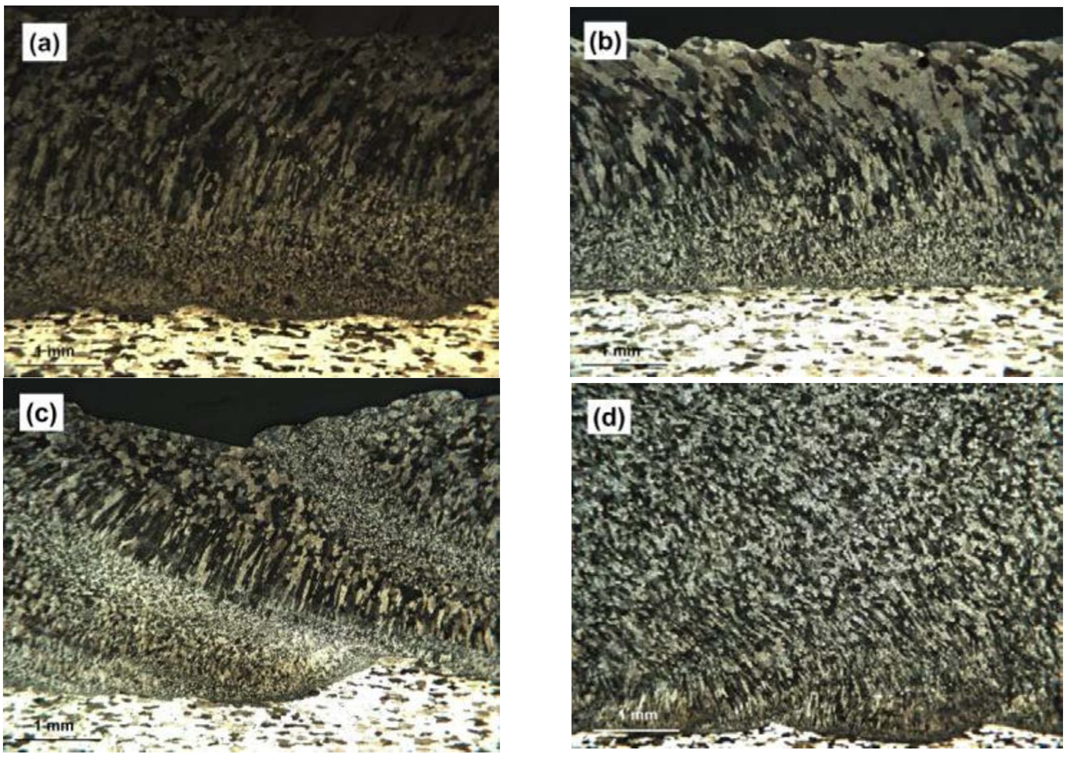

Figure 20 Weld microstructure of (a) Conventional CMT (b) CMT-P (c) CMT-ADV and (d) CMT-PADV(50)

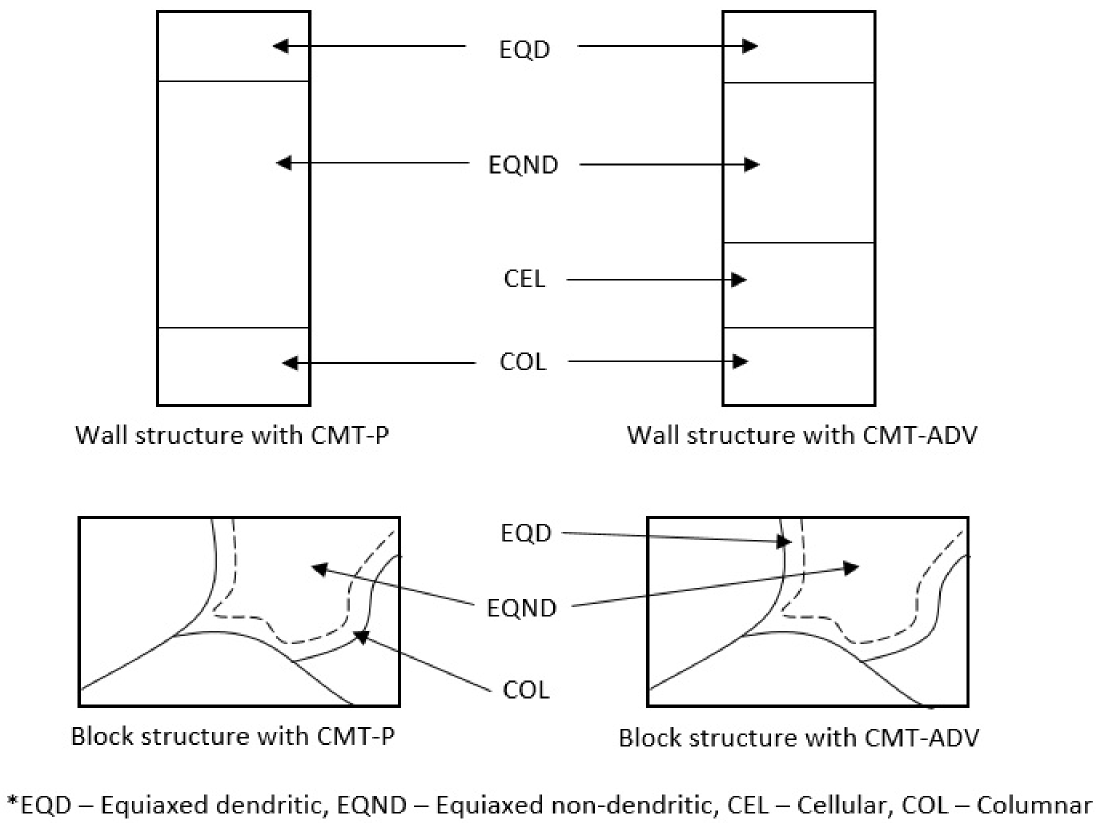

Figure 21 Schematic of microstructure variation in wall and block structure using CMT-P and CMT-ADV processes

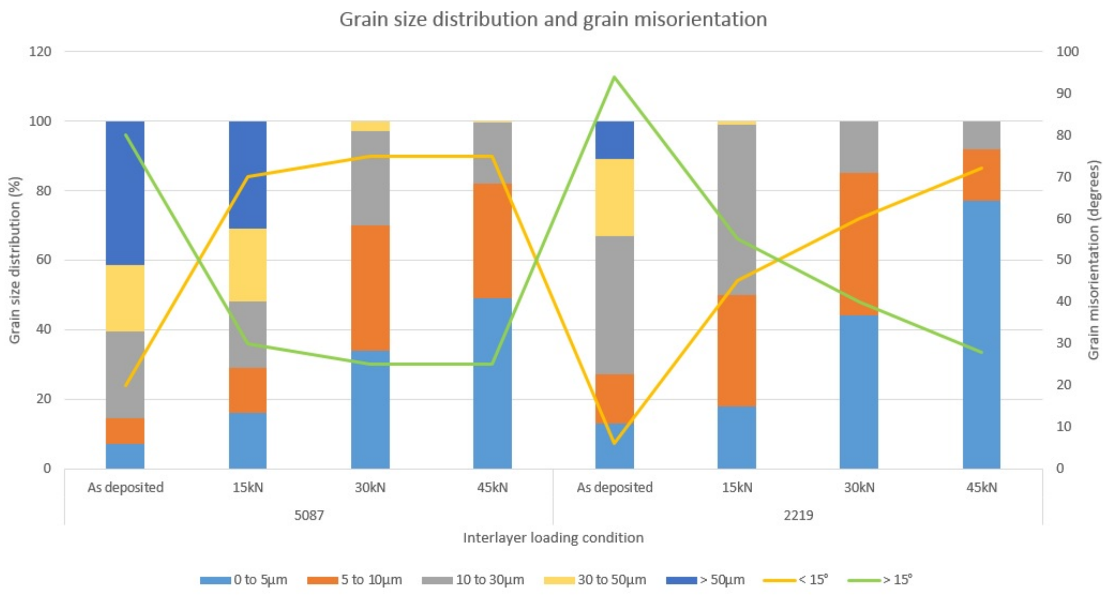

Figure 22 Effect different interlayer rolling conditions on grain size distribution and grain orientation in 5087 and 2219 alloys

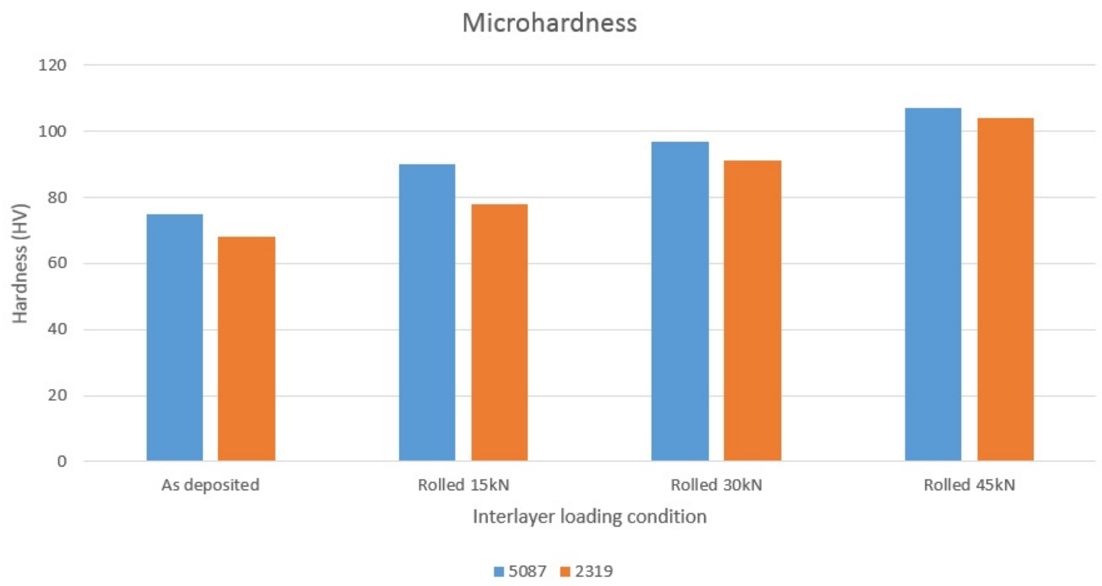

Figure 23 Effect of interlayer rolling with different loads on microhardness